HOKKAIDO UNIVERSITY

Title	Purine nucleotide biosynthesis pathway as a drug target : Identification of novel IMPDH and GMPR from Trypanosoma congolense, and an inhibitor screening study of Cryptosporidium parvum and human type II IMPDH
Author(s)	Sarwono, Albertus Eka Yudistira
Degree Grantor	北海道大学
Degree Name	博士(農学)
Dissertation Number	甲第13324号
Issue Date	2018-09-25
DOI	https://doi.org/10.14943/doctoral.k13324
Doc URL	https://hdl.handle.net/2115/82798
Type	doctoral thesis
File Information	Albertus_Eka_Yudistira_Sarwono.pdf

Hokkaido University Collection of Scholarly and Academic Papers : HUSCAP

Purine nucleotide biosynthesis pathway as a drug target: Identification of novel IMPDH and GMPR from *Trypanosoma congolense*, and an inhibitor screening study of *Cryptosporidium parvum* and human type II IMPDH

（薬物標的としてのプリンヌクレオチド生合成：*Trypanosoma congolense* 由来の新規 IMPDH 及び GMPR の同定,並びに *Cryptosporidium parvum* 及びヒト II 型 IMPDH　阻害剤の探索研究）

ALBERTUS EKA YUDISTIRA SARWONO

Doctor Course

Laboratory of Wood Chemistry and Chemical Biology

Division of Applied Bioscience

Graduate School of Agriculture

Hokkaido University

CONTENTS

ABBREVIATIONS vi

FIGURES vii

TABLES ix

CHAPTER I. GENERAL INTRODUCTION 1

1. Purine nucleotide biosynthesis in the biological system 1

2. Purine nucleotide biosynthesis as a drug target 2

2.1. Targeting the biosynthesis pathway in human cells 3

2.2. Targeting the biosynthesis pathway in microbial cells 4

3. Conclusion 5

CHAPTER II. IDENTIFICATION AND CHARACTERIZATION OF *TRYPANOSOMA CONGOLENSE* GMPR AND IMPDH 6

1. INTRODUCTION 6

1.1. *Trypanosoma congolense* and *nagana* disease 6

1.2. Purine nucleotide biosynthesis in *T. congolense* 7

1.3. Identification of GMPR and IMPDH of *T. congolense* 8

2. MATERIALS AND METHODS 9

2.1. Homology and phylogenic analysis of GMPRs and IMPDHs 9

2.2. Expression of recombinant TcIL3000_5_1940 9

2.3. Purification of recombinant TcIL3000_5_1940 9

2.4. Enzymatic characterization of TcIL3000_5_1940 10

2.5. Effect of temperature to TcGMPR activity 10

2.6. Effect of pH to TcGMPR activity 11

2.7. Kinetic parameter determination of TcGMPR 11

2.8. Inhibition of TcGMPR by MPA 11
2.9. Activation of TcGMPR by monovalent cation 12
2.10. Reverse reaction of TcGMPR 12
2.11. Expression, purification, and enzymatic characterization of BAT33662.1 12
2.12. Inhibition of TcIMPDH by MPA 12
3. RESULTS AND DISCUSSION 14
3.1. Bioinformatics analysis of TcIL3000_5_1940 14
3.2. Enzymatic identification of TcIL3000_5_1940 19
3.3. Effect of temperature to TcGMPR activity 20
3.4. Effect of pH to TcGMPR activity 21
3.5. Enzymatic analysis of TcGMPR 22
3.6. Inhibition of TcGMPR by mycophenolic acid 24
3.7. Activation of TcGMPR by monovalent cation 25
3.8. Reverse reaction of GMPR 27
3.9. Identification of BAT33662.1, an TcIL3000_5_1940 orthologue 28
3.10. Inhibition of TcIMPDH by MPA 30
3.11. A distinction point between GMPR and IMPDH 31
4. CONCLUSION 33
CHAPTER III. HIGH THROUGHPUT SCREENING FOR IMPDH INHIBITORS 34
1. INTRODUCTION 34
1.1. The role of IMPDH in various diseases 34
1.2. The significance of human IMPDH 34
1.3. The significance of *Cryptosporidium parvum* IMPDH 34
1.4. High Throughput Screening 36
1.5. High Throughput Screening of IMPDH inhibitors 37
2. MATERIAL AND METHODS 39

2.1. Molecular methods 39
2.2. Expression and purification of recombinant IMPDH 39
2.3. Determination of enzyme kinetic parameter of CpIMPDH and hIMPDH II 39
2.4. High-Throughput Screening of IMPDH inhibitors 40
2.5. Dialysis for determination of inhibition reversibility 41
2.6. Kinetics of IMPDH inhibition by hit compounds 41
2.6.1. Irreversible inhibition 41
2.6.2. Reversible inhibition 42
2.7. Molecular docking of IMPDH inhibitors 43
2.7.1. Preparation of small molecule ligands 43
2.7.2. Preparation of protein 43
2.7.3. Molecular docking 44
3. RESULTS AND DISCUSSION 45
3.1. Analysis of CpIMPDH and hIMPDH II isolates 45
3.2. HTS of chemical library compounds 47
3.2.1. The first screening 47
3.2.2. Reproducibility assay 49
3.2.3. Dose-dependency assay 50
3.2.4. The second screening: Counter assay 52
3.2.5. Final hit compounds 54
3.3. Analysis of the hit compounds 55
3.3.1. Measurement of IC_{50} values against CpIMPDH and hIMPDH 55
3.3.2. Determination of inhibition irreversibility 59
3.4. The analysis of IMPDH inhibition by disulfiram and bronopol 61
3.4.1. Substrate protection analysis of disulfiram and bronopol 61
3.4.2. The kinetics of irreversible inhibition by disulfiram and bronopol 62
3.5. The analysis of IMPDH inhibition by ebselen 66

3.5.1. The kinetics of reversible CpIMPDH inhibition by ebselen 66
3.5.2. Substrate protection analysis of ebselen 69
3.5.3. The kinetics of irreversible hIMPDH II inhibition by ebselen 70
3.6. Docking of hit compounds to hIMPDH II 72
3.7. Inhibition of GMPR by the hit compounds 73
4. CONCLUSION 75
5. PUBLICATIONS AND CONFERENCES 76
ACKNOWLEDGEMENT 78
REFERENCES 79
APPENDIXES 92

ABBREVIATIONS

AMP	:	adenosine monophosphate
DTT	:	dithiothreitol
GMP	:	guanosine-5'-monophosphate
GMPR	:	guanosine-5'-monophosphate reductase
GMPS	:	guanosine-5'-monophosphate synthase
GST	:	glutathione *S*-transferase
HTS	:	high throughput screening
IC_{50}	:	half-maximum inhibitory concentration
IMP	:	inosine-5'-monophosphate
IMPDH	:	inosine-5'-monophosphate dehydrogenase
kDa	:	kilo Dalton
MPA	:	mycophenolic acid
NAD^+	:	nicotinamide adenine dinucleotide
NADH	:	reduced nicotinamide adenine dinucleotide
$NADP^+$	:	nicotinamide adenine dinucleotide phosphate
NADPH	:	reduced nicotinamide adenine dinucleotide phosphate
RLU	:	relative luminescence unit
SDS-PAGE	:	sodium dodecyl sulfate-polyacrylamide gel electrophoresis
XMP	:	xanthosine monophosphate

FIGURES

Fig. 1. The general scheme of minimal purine nucleotide biosynthesis pathway **1**

Fig. 2. Catalytic reaction of GMPR **2**

Fig. 3. Catalytic reaction of IMPDH **2**

Fig. 4. Purine nucleotide biosynthesis in a protozoan infection model **4**

Fig. 5. *Trypanosoma congolense* in blood smear **6**

Fig. 6. Phylogenetic tree for TcIL3000_5_1940. ..... **14**

Fig. 7. Amino acid alignment of TcIL3000_5_1940 (target) in comparison to GMPRs. **18**

Fig. 8. SDS-PAGE of recombinant TcIL3000_5_1940. ..... **19**

Fig. 9. Enzymatic identification of TcIL3000_5_1940 ..... **20**

Fig. 10. Determination of optimum temperature for TcGMPR **21**

Fig. 11. Determination of optimum pH for TcGMPR **22**

Fig. 12. Steady-state kinetic analysis of TcGMPR **23**

Fig. 13. The structure of mycophenolic acid **25**

Fig. 14. Inhibitory activity of MPA against TcGMPR **25**

Fig. 15. Effect of monovalent cation on TcGMPR **26**

Fig. 16. Reverse reaction of GMPR **27**

Fig. 17. Phylogenetic tree for BAT33662.1. ..... **28**

Fig. 18. Enzymatic identification of BAT33662.1 ..... **29**

Fig. 19. Amino acid sequence of the novel TcIMPDH **30**

Fig. 20. Inhibitory activity of MPA to TcIMPDH **30**

Fig. 21. The distinction point between GMPRs and IMPDHs **32**

Fig. 22. *Cryptosporidium parvum* oocyst with Ziehl-Neelson staining **35**

Fig. 23. Chemotherapeutic agents for cryptosporidiosis **36**

Fig. 24. Luminescence detection of IMPDH activity **38**

Fig. 25. Kinetic determination of CpIMPDH **45**

Fig. 26. Kinetic determination of hIMPDH II **46**

Fig. 27. Scheme of assay plates in the first screening **48**

Fig. 28. Heatmap of the first screening **49**

Fig. 29. Reproducibility assay of hit compounds. **50**

Fig. 30. The twenty-nine compounds with IC_{50} less than 10 μM. 51

Fig. 31. Inter-relation model of counter assay 53

Fig. 32. Synergistic model of counter assay 54

Fig. 33. The structures of the hit compounds 55

Fig. 34. Dose-dependency inhibition of hit compounds 56

Fig. 35. Shift of IC_{50} after incubation with DTT 58

Fig. 36. Dialysis experiment for detection of inhibition irreversibility 60

Fig. 37. Substrate protection against disulfiram and bronopol 61

Fig. 38. Decay of enzyme activity in the presence of disulfiram and bronopol 63

Fig. 39. The inactivation of IMPDH by disulfiram and bronopol. 64

Fig. 40. One-step inactivation of enzyme 64

Fig. 41. Ebselen reversibly inhibit CpIMPDH. 67

Fig. 42. Kinetics of ebselen inhibition of CpIMPDH. 68

Fig. 43. Substrate protection against ebselen 69

Fig. 44. The inactivation of hIMPDH II by ebselen 71

Fig. 45. Molecular docking of hit compounds to hIMPDH II 72

Fig. 46. Dose-dependent inhibition of hit compounds against TcGMPR 74

TABLES

Table 1. Amino acid sequence of target protein compared to GMPRs **16**

Table 2. Amino acid sequence of target protein compared to IMPDHs **17**

Table 3. Comparison of enzymatic parameters of TcGMPR to other GMPR **24**

Table 4. Kinetics of CpIMPDH **46**

Table 5. Kinetics of hIMPDH II **46**

Table 6. IC_{50} of the hit compounds **59**

Table 7. Substrate protection against disulfiram and bronopol in CpIMPDH **62**

Table 8. k_{on} values of disulfiram and bronopol inhibition against IMPDHs **65**

Table 9. Kinetics of ebselen inhibition against CpIMPDH **68**

Table 10. Substrate protection against ebselen inactivation in hIMPDH II **70**

Table 11. k_{on} values of ebselen against hIMPDHs **71**

CHAPTER I. GENERAL INTRODUCTION

1. Purine nucleotide biosynthesis in the biological system

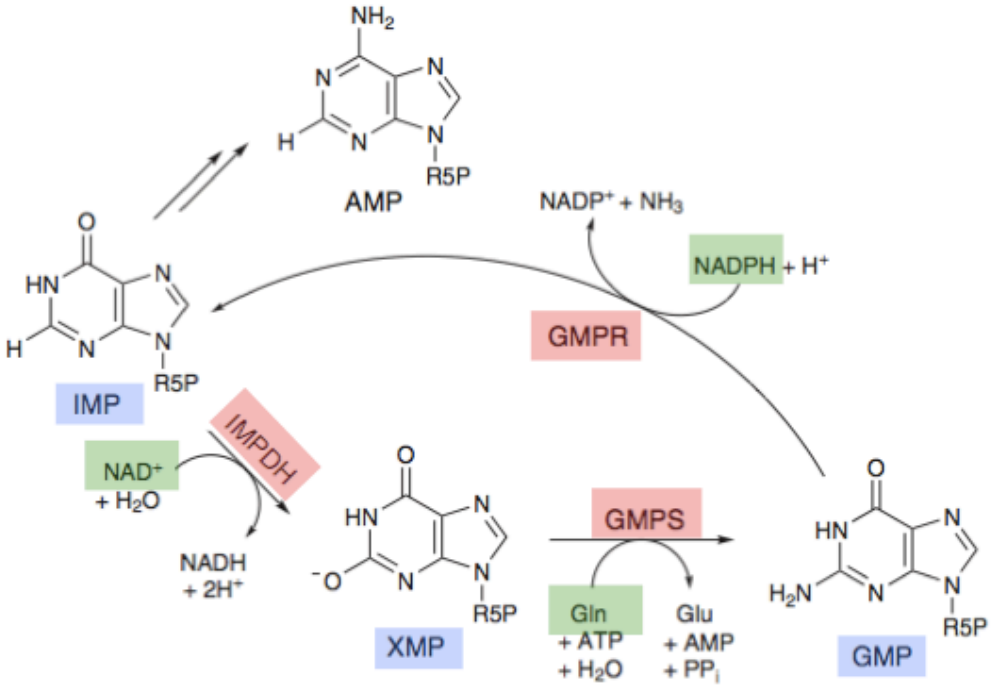


Fig. 1. The general scheme of minimal purine nucleotide biosynthesis pathway (Hedstrom, 2009)

Purine nucleotide is an essential building block for genetic material syntheses in nearly all organisms. The simplest machinery of purine nucleotide biosynthesis pathway involves three essential enzymes: guanosine 5'-monophosphate dehydrogenase (GMPR) (EC 1.7.1.7), inosine 5'-monophosphate dehydrogenase (IMPDH) (EC 1.1.1.205), and GMP synthase (GMPS) (EC 6.3.5.2), with each catalyzing the conversion of GMP to IMP, IMP to XMP, and XMP back to GMP, respectively (Fig. 1). These enzymes cooperatively regulate and maintain the intracellular balance of adenosine monophosphate (AMP) and guanosine monophosphate (GMP).

These enzymes share some conserved regions in their primary structure, partly due to the similarity in reactions they carry out. Consequently, misannotations between these

enzymes are common, particularly between GMPR and IMPDH (Figs. 2 and 3). Therefore, the annotation of an enzyme of GMPR/IMPDH family should not be performed only by a BLAST search (Hedstrom, 2012). The most striking similarities between IMPDH and GMPR were found in Kinetoplastida genome, where both enzymes apparently have a cystathionine *β*-synthase (CBS) pair domain in its structure. Previously, the domain was only found in IMPDHs, thus regarded as a characteristic of this class of enzyme (Bessho *et al.*, 2016; Smith *et al.*, 2016).

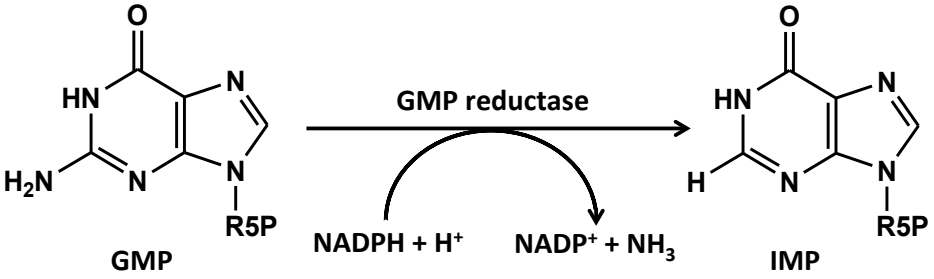


Fig. 2. Catalytic reaction of GMPR

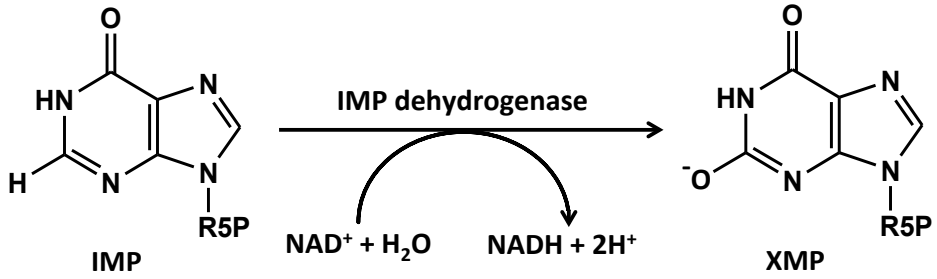


Fig. 3. Catalytic reaction of IMPDH

2. Purine nucleotide biosynthesis as a drug target

Due to their essential role in nucleic acid biosynthesis, the enzymes in the purine nucleotide biosynthesis pathway are considered as an important drug targets. The inhibition of IMPDH, GMPR, or GMPS has been proved as one of the chemotherapeutic

strategies against various medical conditions (Hammond & Gutteridge, 1984; Wang *et al.*, 1996; Jain *et al.*, 2001; Chaudhary *et al.*, 2004; Umejiego *et al.*, 2004; Xu *et al.*, 2017).

2.1. Targeting the biosynthesis pathway in human cells

In human, there are two isoform of IMPDH: human IMPDH type I (hIMPDH I) and type II (hIMPDH II). The former has been associated with the homeostasis maintenance of various biochemical processes in the body. This isoform generally expressed in a low level by various tissues, mainly in retina, spleen, and peripheral blood mononuclear cells. In contrast, hIMPDH II is expressed more dominantly in the actively replicating cells (Hedstrom, 2009).

Due to its role, hIMPDH II has been considered as a potential drug target for the treatment of various medical conditions. The inhibitors of hIMPDH II specifically have been investigated as chemotherapeutic agents for controlling the progression of cancer cells, proliferation of lymphocyte cells, and replication of invading viruses. These bioactivities have been proven as the consequence of the depletion in guanine nucleotide pool. The broad application of hIMPDH II inhibitors therefore justified the screening effort for discovering more potent inhibitors against the enzyme.

2.2. Targeting the biosynthesis pathway in microbial cells

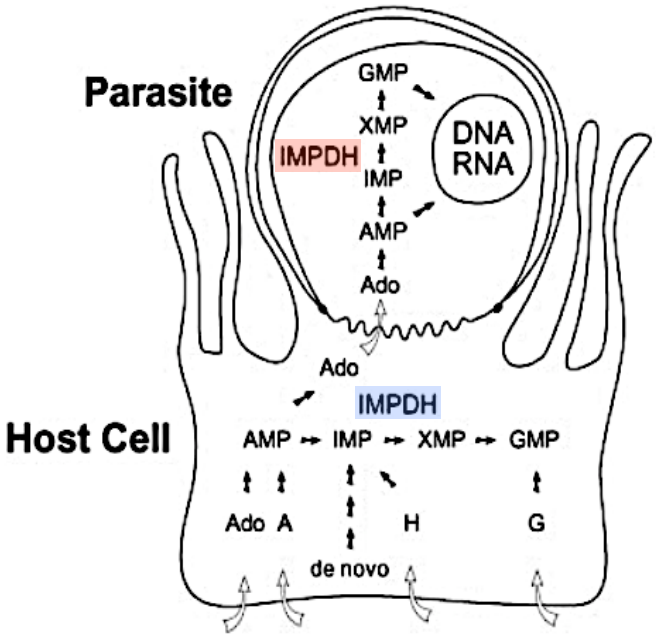


Fig. 4. Purine nucleotide biosynthesis in a protozoan infection model (Umejiego *et al.*, 2004)

Ado: adenosine; A: adenine; H: hypoxanthine; G: guanine

Generally, there are two pathways for biosynthesis of nucleotides: *de novo* and salvage pathway. In *de novo* synthesis, the nucleotide bases are synthesized from simpler compounds, which then attached to a ribose-based structure. Salvage pathway, on the other hand, relies on the recovery process of a preformed nucleotide bases, which then attached to a ribose unit (Berg *et al.*, 2002). For most organism, purine nucleotide biosynthesis could be carried out in several different pathways, both *de novo* and salvage. However, microbe from phylum Apicomplexa, such as pathogenic protozoan Cryptosporidium spp., relies solely on a very simple and streamlined salvage pathway to produce its guanosine nucleotides (Fig. 4). This difference lays the basis for the development of apicomplexan IMPDH as a molecular target for anti-protozoan agent.

Generally, inhibition in one of the enzymes on the purine biosynthesis pathway of an apicomplexan pathogen could halt the nucleic acid synthesis in the parasite cell, thus harmful to the organism (Hammond & Gutteridge, 1984; Chaudhary *et al.*, 2004; Ullman *et al.*, 2008). Interestingly, many other microbes supposedly having *de novo* purine biosynthesis pathway also showed a growth inhibition in the presence of IMPDH inhibitors, indicating the reliance of the microbes to the salvage pathway (Hedstrom *et al.*, 2011). Therefore, the discovery of selective inhibitor against microbial IMPDH is necessary.

3. Conclusion

Due to the significance of the purine biosynthesis pathway, it is essential to completely characterize the kinetics and inhibition properties of the enzymes involved in this pathway, both for mammalian enzymes and microbial enzymes. Furthermore, studying the enzymes in the inter- and intra-species setting is necessary in order to develop more selective inhibitors.

CHAPTER II. IDENTIFICATION AND CHARACTERIZATION OF *TRYPANOSOMA CONGOLENSE* GMPR AND IMPDH

1. INTRODUCTION

1.1. *Trypanosoma congolense* and *nagana* disease

T. congolense is an economically important pathogenic protozoan in tropical part of Africa. The protozoa infect a broad range of African animals, inflicting fatal animal trypanosomosis, which is also known as *nagana* disease. A study has described the infection of *T. congolense* in domesticated animals in central Africa as one of the determining factors that hinders the financial development of the society (Noyes *et al.*, 2011).

T. congolense itself is the smallest of all pathogenic trypanosomes, with length between 9-22 μm (Fig. 5). The life cycle of this parasite includes a phase in mammal bloodstream and a phase in the vector, tse-tse fly (*Glossina* sp.).

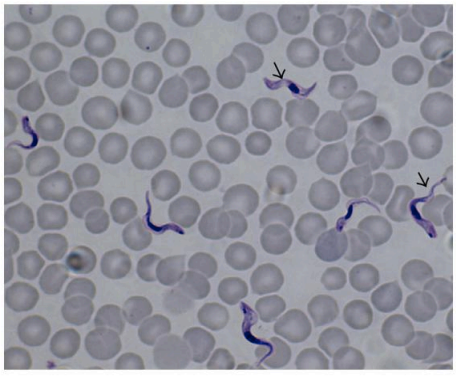


Fig. 5. *Trypanosoma congolense* in blood smear (Munang'Andu *et al.*, 2012)

The infection of *T. congolense* to mammals was initiated by the bite of infected tse-tse flies. The protozoa depend solely on its vector for completing its life in mammalian

blood. Therefore, the incidents of *T. congolense* infection were confined very closely to the tse-tse habitat (FAO, 2014).

Current chemotherapeutic compounds used against *T. congolense* infection consist of relatively old and low-efficacious compounds, resulting in the emergence of chemo-resistant *T. congolense* strains (Codjia *et al.*, 1993; Mamoudou *et al.*, 2008; Chitanga *et al.*, 2011). The discovery of novel chemotherapeutic agents against trypanosomosis also suffered from limited attention and funding from major pharmaceutical companies (Delespaux *et al.*, 2010; Matthews, 2015).

Naturally, humans are resistant to *T. congolense* infection due to the trypanosome lytic factor in the serum. However, some cases of *T. congolense* infection in human have also been reported. While the exact mechanism underlying these cases are yet to be explained, the incidents have highlighted the possibility of future outbreak of infection in human (Hawking, 1978; Joshua, 1989; Truc *et al.*, 2013). Therefore, it is of a high importance not only to discover new drug compounds but also to identify new druggable molecular targets.

1.2. Purine nucleotide biosynthesis in *T. congolense*

Similar to some protozoa, *T. congolense* relies on a salvage pathway to produce purine nucleotides in its cell (Hammond & Gutteridge, 1984; McConkey, 2000; Li *et al.*, 2015; Bessho *et al.*, 2016; Boitz, Jardim & Ullman, 2016). The enzymes involved in this pathway were mostly detected in the glycosomes (Vertommen *et al.*, 2008; Sarwono *et al.*, 2017). Some reports have confirmed that an inhibition against one of the enzymes involved in the pathway could effectively inhibit the proliferation of pathogens relying on this pathway. This validates the pathway as a promising drug target for anti-trypanosomal chemotherapy (McConkey, 2000; Umejiego *et al.*, 2004; Hedstrom, 2009; Liechti & Goldberg, 2012; Cao *et al.*, 2013; Gorla *et al.*, 2014; Li *et al.*, 2015; Smith *et al.*, 2016).

However, up to the current time, this pathway has not been explored as a chemotherapeutic target against *T. congolense* infection. In fact, the GMPR, IMPDH, and GMPS of *T. congolense* have yet to be identified and characterized.

1.3. Identification of GMPR and IMPDH of *T. congolense*

This study was aimed to identify and characterize the unique GMPR and IMPDH-encoding genes in *T. congolense*. Previously, a BLAST search of IMPDH analogues in *T. congolense* genome resulted in a match with a protein encoded by TcIL3000_5_1940. Interestingly, this particular enzyme has been annotated both as IMPDH and as GMPR, a typical annotation discrepancy on this enzyme family. Furthermore, BAT33662.1, an analogue of TcIL3000_5_1940, was also found in a sequencing study in *T. congolense* genome. Enzymatic activity of both enzymes was investigated in this study.

Firstly, TcIL3000_5_1940 was expressed in *E. coli* and subjected to both IMPDH and GMPR assay to confirm its identity. Having confirmed the identity of the enzyme, kinetic experiments were conducted on the protein. Secondly, the inhibition of the enzyme by mycophenolic acid, a selective IMPDH inhibitor, was investigated. The primary structure of the protein was then compared to other proteins in the IMPDH/GMPR family to discover a distinctive group of amino acid between GMPR and IMPDH for more practical enzyme identification.

Next, BAT33662.1 was also analyzed with the same set of experiments. The study of both enzymes is expected to provide beneficial information on *T. congolense* purine biosynthesis for further drug design against trypanosomosis.

2. MATERIALS AND METHODS

2.1. Homology and phylogenic analysis of GMPRs and IMPDHs

A homology analysis was performed using ClustalW version 2.1 (http://clustalw.ddbj.nig.ac.jp). A phylogenetic tree was constructed by neighbor-joining method using MEGA 5.2 software.

2.2. Expression of recombinant TcIL3000_5_1940

The *E. coli* cells harboring TcGMPR-pGEX 6P-2 plasmid were grown in 2xYT broth containing 100 μg/ml ampicillin at 37ºC overnight. The recombinant enzyme, which fused with glutathione *S*-transferase (GST), was induced with 0.1 mM isopropyl thio-*β*-D-galactoside (IPTG) for 12 h at 18ºC. The cells were then harvested, washed with PBS solution, and kept at −80ºC until usage.

2.3. Purification of recombinant TcIL3000_5_1940

The cells were thawed on ice, suspended in 50 mM Tris-HCl pH 8.0 containing 5 mM EDTA (Sigma), 1 mM dithiothreitol (DTT), 0.5 mM phenylmethylsulfonyl fluoride, and 1 μg/ml leupeptin, then sonicated. The cell lysate was centrifuged, and the supernatant was applied to Glutathione Sepharose 4B (GE Healthcare, Bio-Science Corp., UK) overnight. The unbound protein was washed with 30 mM Tris-HCl pH 8.0 containing 1 mM $MgCl_2$, 150 mM NaCl, 1 mM dithiothreitol (DTT), 0.5 mM benzamidine (Sigma-Aldrich Japan, Tokyo, Japan), and 2 μg/ml leupeptin. The GST-tag was cleaved using PreScission protease (GE Healthcare, Bio-Science Corp., UK) according to manufacturer manual. The protein was eluted from the resin by washing with 50 mM Tris-HCl buffer pH 7.5 containing 150 mM NaCl, 1 mM EDTA, and 1 mM DTT. The enzyme-containing eluent was dialyzed overnight with 30 mM Tris-HCl pH 7.5 containing 1 mM $MgCl_2$, 1

mM DTT, 0.5 mM benzamidine, 50% glycerol. All purification processes were carried out at 4°C. The purified IMPDH was then supplemented with 10 μg/ml leupeptin and stored at −20°C until usage. The enzyme concentrations were determined using a Bradford assay. The protein was stored at −80ºC as a 50% glycerol mixture until use.

2.4. Enzymatic characterization of TcIL3000_5_1940

The protein was subjected into both IMPDH and GMPR assay solution. The IMPDH assay solution contains 100 mM KCl, 3 mM EDTA, 1 mM DTT, 0.1 mg/ml BSA, 250 μM IMP, 800 μM NAD^+ in 50 mM Tris-HCl pH 8.0 (25°C). GMPR assay solution contains 100 mM KCl, 3 mM EDTA, 1 mM DTT, 0.1 mg/ml BSA, 100 μM GMP, 100 μM NADPH in 75 mM Tris-HCl pH 7.8 (25°C). The reaction was started by the addition of an appropriate amount of enzyme in a dose-dependent manner. The reaction was carried out for one hour. The production of NADH for IMPDH reaction or the consumption of NADPH for GMPR reaction was monitored by the measurements of OD_{340} using Sunrise Microplate Reader (TECAN, purchased from Wako Pure Chemical Ind., Ltd., Japan).

2.5. Effect of temperature to TcGMPR activity

Briefly, the activity of the recombinant protein was measured in 75 mM Tris-HCl pH 7.0 buffer under various temperatures (25-45ºC). The reaction solution contained 200 μM NADPH (Sigma Aldrich, St. Louis, MO, USA), 1 mM GMP (Sigma Aldrich Japan, Tokyo, Japan), 100 mM KCl, 3 mM EDTA, 0.1 mg/ml bovine serum albumin (BSA), and 1 mM dithiothreitol. The ionic strength of the solution was set to 0.2 with NaCl. The enzyme assay was started by the addition of TcGMPR to the reaction solution. Activity of TcGMPR was monitored at 340 nm using Biophotometer plus spectrophotometer (Eppendorf, Germany) to measure the conversion of NADPH to $NADP^+$. Activity for each

pH value was expressed as percent difference of initial velocity (V_0) value from V_0 at pH 7.0.

2.6. Effect of pH to TcGMPR activity

The experiment was conducted similarly as optimum temperature experiment. The activity of the recombinant protein was measured at 35ºC in 75 mM Tris-HCl buffer under various pH conditions (7.0-8.7).

2.7. Kinetic parameter determination of TcGMPR

The kinetic parameters of the enzyme were measured with an assay solution containing 75 mM Tris-HCl pH 7.0, 100 mM KCl, 3 mM EDTA, 1 mM DTT, and 0.1 mg/ml BSA at 35ºC. The ionic strength of the solution was set to 0.2 with NaCl. Various concentrations of GMP were used with a fixed dose of NADPH at 200 μM for measurement of steady-state kinetics against GMP. In the measurement of steady-state kinetics against NADPH, various concentrations of NADPH were used with fixed dose of GMP at 1 mM. Measurements of V_{max} and K_m were conducted by fitting the acquired initial velocity data to the Michaelis-Menten equation using GraFit 7 software (Erithacus software, UK).

2.8. Inhibition of TcGMPR by MPA

The inhibition of MPA to TcGMPR was measured with an assay solution containing 75 mM Tris-HCl pH 7.0, 100 mM KCl, 3 mM EDTA, 1 mM DTT, 0.1 mg/ml BSA, 100 μM NADPH, 100 μM GMP, and various concentrations of MPA at 30ºC. DMSO was used as vehicle, with a final concentration of 1%. The reaction was started by adding 50 nM of TcGMPR. The reaction was carried out for 1 h. Activity of TcGMPR was

monitored as a decrease of absorbance at 340 nm. Each point was expressed as a percentage of consumed NADPH in each treatment sample relative to the control vehicle. The IC_{50} value was calculated using GraFit 7 software.

2.9. Activation of TcGMPR by monovalent cation

Enzyme activation by monovalent cation was conducted with an assay solution containing 75 mM Tris-HCl pH 7.0, 3 mM EDTA, 1 mM DTT, 0.1 mg/ml BSA, 200 μM NADPH, 1 mM GMP, and 100 mM monovalent chloride (either LiCl, NaCl, KCl, CsCl, or NH_4Cl) at 35ºC. Activity for each monovalent cation was expressed as a percent difference of the initial velocity (V_0) value from V_0 in the assay with NaCl.

2.10. Reverse reaction of TcGMPR

The assay of GMPR reverse reaction activity was conducted with solution containing 75 mM Tris-HCl pH 8.0, 100 mM KCl, 3 mM EDTA, 1 mM DTT, 1 mM $NADP^+$, 50 mM NH_4Cl, and various IMP concentrations. Reaction was initiated by addition of enzyme to the assay solution. The reaction was carried out at 25ºC for 20 h. The reverse GMPR activity was monitored as an increase of OD_{340}, indicating the formation of NADPH.

2.11. Expression, purification, and enzymatic characterization of BAT33662.1

Expression and purification was conducted as section 2.2, 2.3, and 2.4.

2.12. Inhibition of TcIMPDH by MPA

The inhibition of MPA to TcIMPDH was measured with an assay solution containing 50 mM Tris-HCl pH 8.0, 100 mM KCl, 3 mM EDTA, 1 mM DTT, 0.1 mg/ml BSA, 250 μM IMP, 800 μM NAD^+, and various concentrations of MPA at 30ºC. DMSO

was used as vehicle, with a final concentration of 1%. The reaction was started by adding 40 nM of TcIMPDH. The reaction was carried out for 1 h. Activity of TcIMPDH was monitored as an increase of absorbance at 340 nm. The IC_{50} value was calculated using GraFit 7 software.

3. RESULTS AND DISCUSSION

3.1. Bioinformatics analysis of TcIL3000_5_1940

The similarity of the amino acid sequences between GMPRs and IMPDHs often resulted in misannotations between the enzymes. This case highlighted the flaw of enzyme identification process only by utilizing the gene BLAST alignment (Hedstrom, 2012). Conventionally, IMPDHs and GMPRs were classified into different clades in the phylogenetic tree, with the CBS domain as the key distinctive point to characterize IMPDH. However, the CBS domain was also found in the GMPR from *L. donovani* and *T. brucei* (Spector & Jones, 1982; Bessho *et al.*, 2016). TcIL3000_5_1940 itself was classified in the same clade as *L. donovani* and *T. brucei* GMPR as shown in Fig. 6.

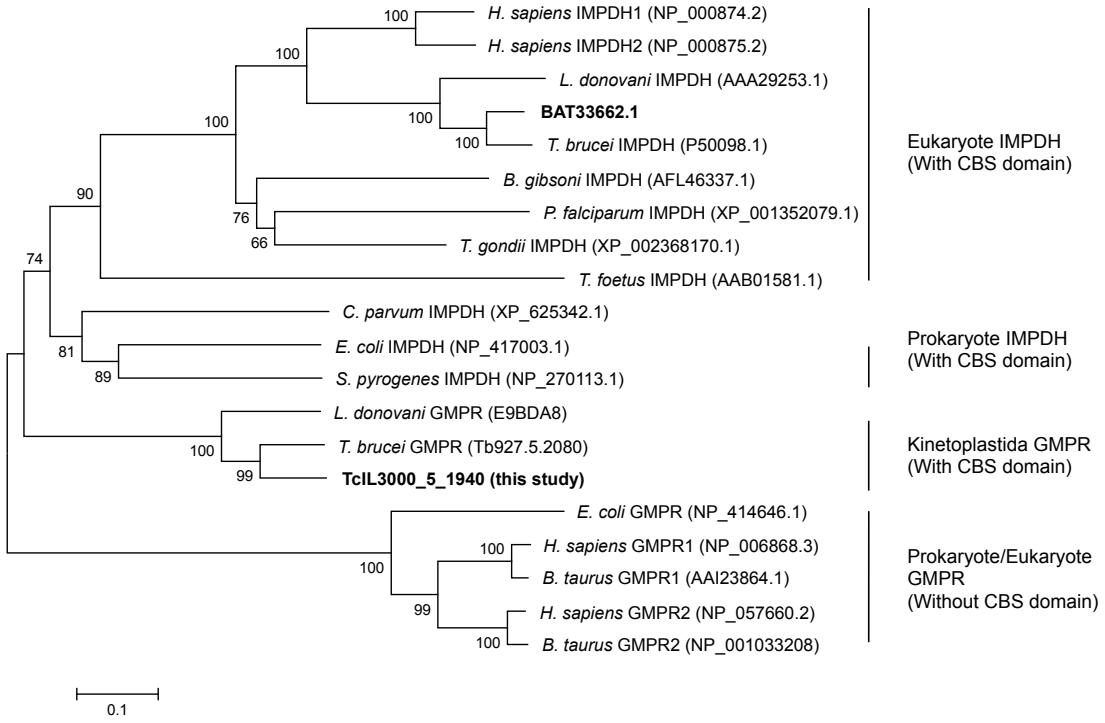


Fig. 6. Phylogenetic tree for TcIL3000_5_1940.

The CBS domain is actually not a core catalytic point for the enzymatic activity. However, it may act as a regulatory domain to bind ATP, AMP, AdoMet, and so on

(Ignoul & Eggermont, 2005). In a report on *Leishmania* GMPR, CBS has been linked to biological responses of GMPR at the intracellular level of GTP and ATP, which subsequently controls the state of the enzyme complex to modulate its catalytic activity (Smith *et al.*, 2016).

TcIL3000_5_1940 itself shares high degree of similarity in amino acid sequence with GMPR from other Kinetoplastide *L. donovani* and *T. brucei* with similarity of 72% and 80%, respectively. However, TcIL3000_5_1940 shares only 32-35% gene similarity to human GMPR1 (HsGMPR1), HsGMPR2, and *Bos taurus* GMPR1 (BtGMPR), and BtGMPR2 as indicated in Table 1 (Andrews & Guest, 1988; Kondoh *et al.*, 1991; Deng *et al.*, 2002; Martinelli *et al.*, 2011; Bessho *et al.*, 2016). In contrast, there are up to 44% of shared identity in the primary structures between TcIL3000_5_1940 and the IMPDHs in this study (Table 2). Inferred from these findings, TcIL3000_5_1940 was expected to be a GMPR, and not an IMPDH (Fig. 7).

Table 1. Amino acid sequence of target protein compared to GMPRs

	Identity (%)						
	TcIL3000_5_1940	*T. brucei* GMPR	*L. donovani* GMPR	*H. sapiens* GMPR1	*H. sapiens* GMPR2	*B. taurus* GMPR1	*B. taurus* GMPR2
TcIL3000_5_1940	100	80	72	34	32	35	34
T. brucei GMPR		100	72	34	32	35	33
L. donovani GMPR			100	32	31	32	31
H. sapiens GMPR1				100	79	95	79
H. sapiens GMPR2					100	80	94
B. taurus GMPR1						100	79
B. taurus GMPR2							100

Identities were calculated using ClustalW program.

Table 2. Amino acid sequence of target protein compared to IMPDHs

Protein sequence	Identity (%)
TcIL3000_5_1940	100
T. congolense IMPDH	34
T. brucei IMPDH	34
L. donovani IMPDH	33
S. pyrogenes IMPDH	41
E. coli IMPDH	39
B. gibsoni IMPDH	33
P. falciparum IMPDH	31
T. gondii IMPDH	37
T. foetus IMPDH	27
C. parvum IMPDH	44
H. sapiens IMPDH1	34
H. sapiens IMPDH2	34

Identities were calculated using ClustalW program.

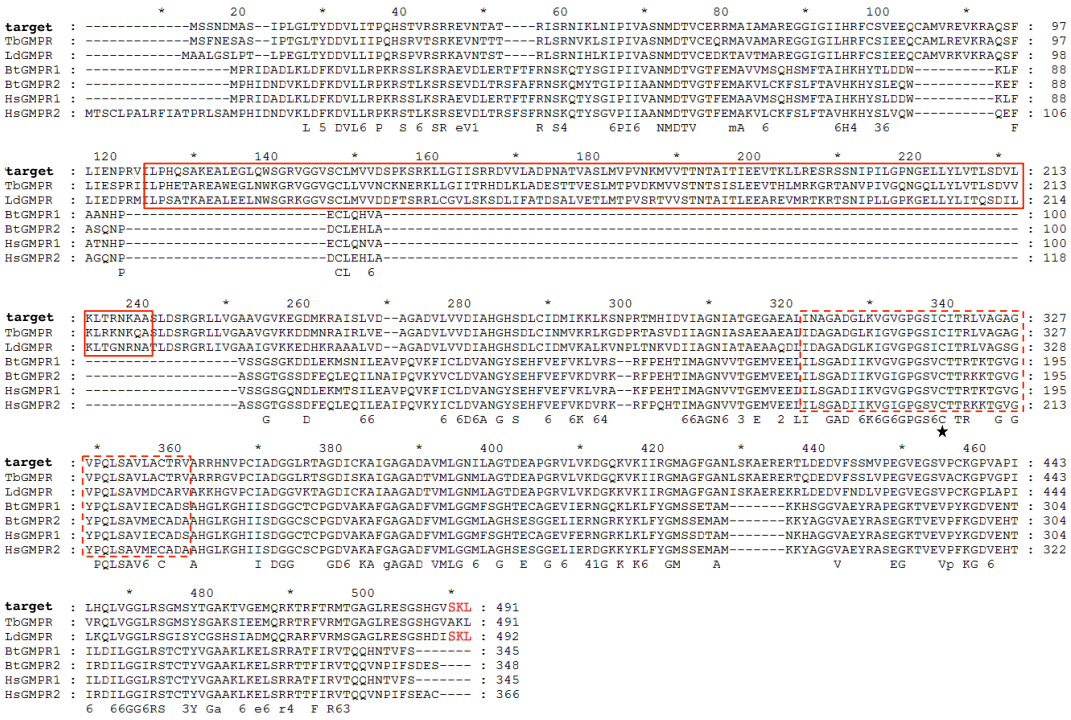


Fig. 7. Amino acid alignment of TcIL3000_5_1940 (target) in comparison to GMPRs.

The square indicates the predicted CBS pair domain amino acid residues. The dashed square indicates the catalytic loop. The red bold characters indicate the C-terminal Ser-Lys-Leu peroxisomal (glycosomal) targeting signal. Star symbol indicates the catalytic Cys204 residue (HsGMPR2 numbering). Protein sequence of target (TriTrypDB: TcIL3000_5_1940); *T. brucei* GMPR [(TbGMPR) TriTrypdDB: Tb927.5.2080]; *L. donovani* GMPR [(LdGMPR) Uniprot: E9BDA8]; *B. taurus* GMPR1 and 2 [(BtGMPR 1) Uniprot: AAI23864.1; (BtGMPR2) NCBI: NP_001033208]; *H. sapiens* GMPR1 and 2 [(HsGMPR1) NCBI: NP_006868.3; (HsGMPR2) NCBI: NP_057660.2] were aligned using ClustalW (http://clustalw.ddbj.nig.ac.jp).

A full length TcIL3000_5_1940 was then cloned and the recombinant protein was expressed in *E. coli*. The purified protein was detected as a single band with a molecular weight of around 52 kDa on SDS-PAGE (Fig. 8).

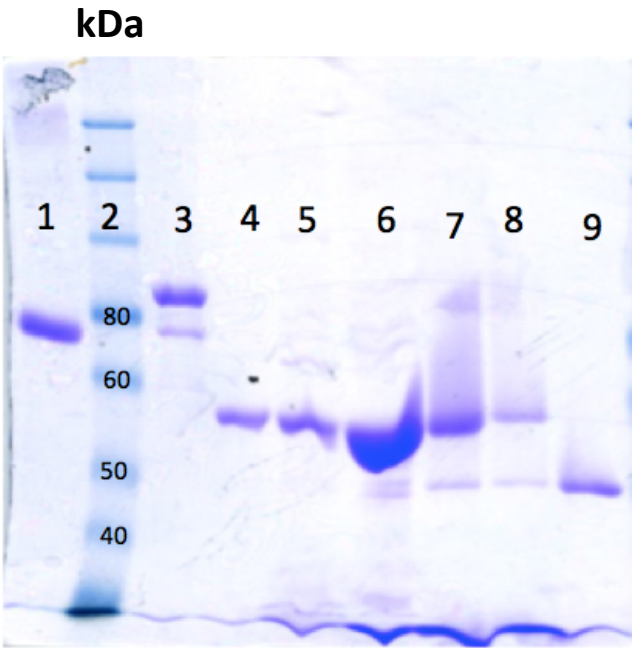


Fig. 8. SDS-PAGE of recombinant TcIL3000_5_1940.

Lane 1: BSA, 2: protein marker, 3: GST-TcIL3000_5_1940, 4,5: TcIL3000_5_1940, 6: post-GST-tag cleaving, 7: First GSH wash of resin bead, 8: Second GSH wash of resin bead, 9: PreScission protease.

3.2. Enzymatic identification of TcIL3000_5_1940

By subjecting the enzyme to both IMPDH and GMPR assay solution, the identity of the protein was determined. hIMPDH II was used as the IMPDH control.

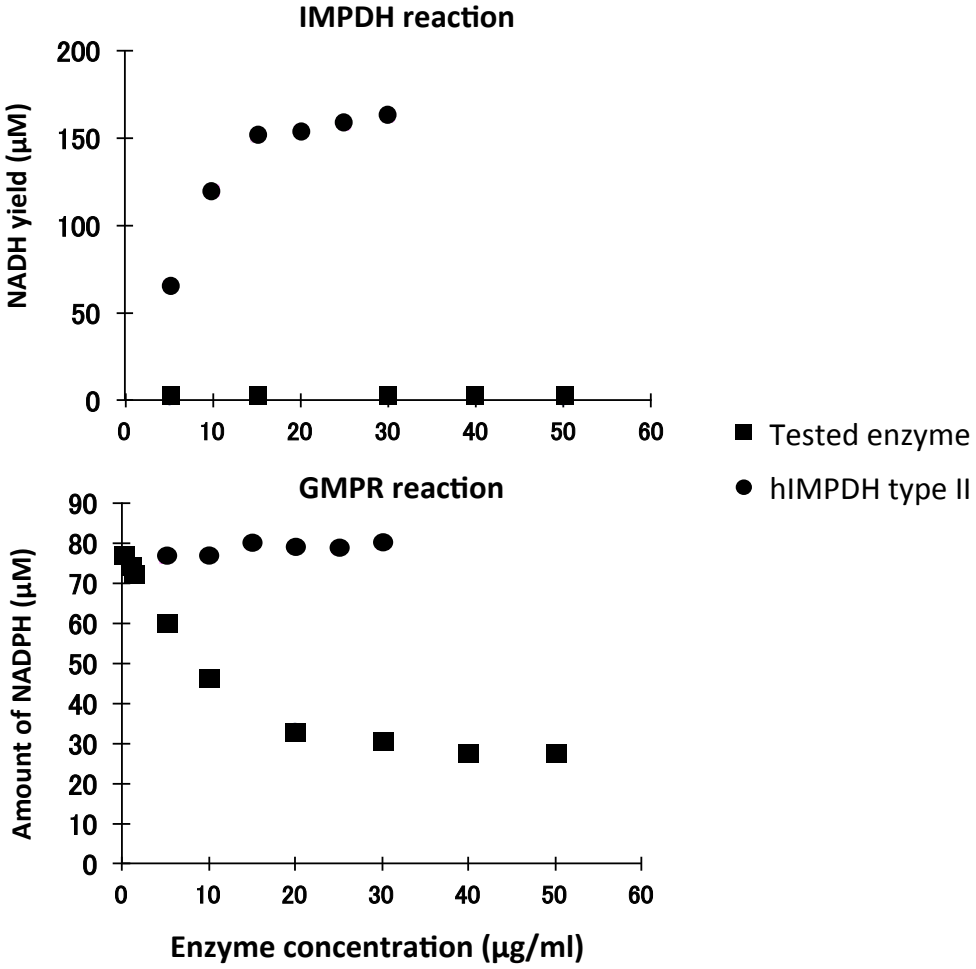


Fig. 9. Enzymatic identification of TcIL3000_5_1940

Unlike hIMPDH II (circles), the TcIL3000_5_1940 (squares) did not produce NADH upon incubation with IMPDH assay solution. In contrast, the incubation in GMPR assay solution resulted in the decrease of NADPH in a dose-dependent manner. Therefore, TcIL3000_5_1940 was identified as a GMPR from *T. congolense* (TcGMPR).

3.3. Effect of temperature to TcGMPR activity

To determine the optimum assay condition for the steady-state kinetics measurement, the activity of the recombinant protein was evaluated at a range of temperature. In agreement with a previous report on *T. brucei* GMPR (TgGMPR), activity of TcGMPR was found to be highest at around 35°C (Fig. 10) (Bessho *et al.*, 2016).

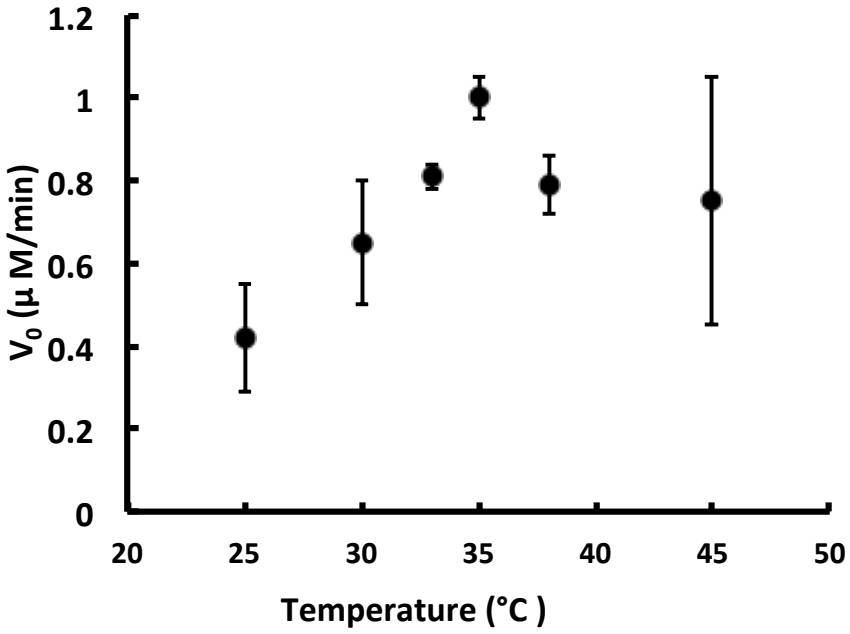


Fig. 10. Determination of optimum temperature for TcGMPR

Each data point represents mean ± standard deviation from three independent experiments.

3.4. Effect of pH to TcGMPR activity

Similar to the determination of optimum temperature, the activity of the recombinant protein was evaluated at several pH values under neutral to basic conditions. Also similar to *T. brucei* GMPR, the activity of TcGMPR was found to be highest at pH 7.0, and gradually decreased as the pH of the assay solution increased (Fig. 11) (Bessho *et al.*, 2016). Acidic conditions are avoided for GMPR studies due to the instability of co-factor NADPH under such conditions.

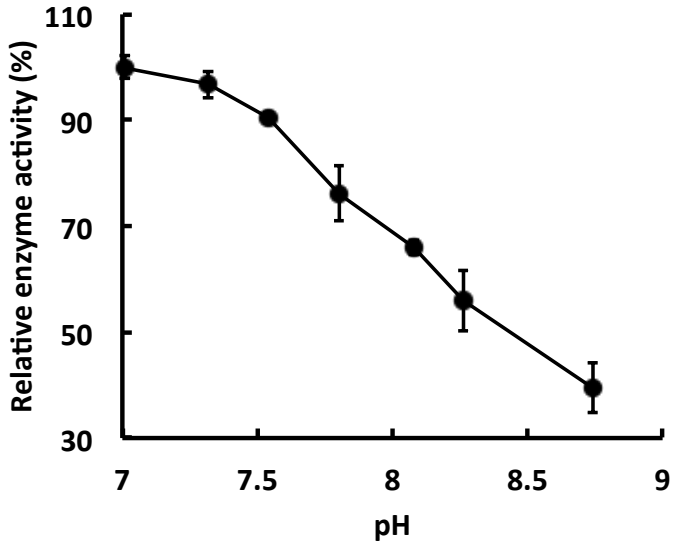


Fig. 11. Determination of optimum pH for TcGMPR

Each TcGMPR activity was plotted against the corresponding value of experimental pH. The activity at pH 7.0 was set as 100% relative activity. Each data point represents mean ± standard deviation from three independent experiments.

3.5. Enzymatic analysis of TcGMPR

By using the predetermined optimum pH and temperature, the kinetic parameters determination was performed. The apparent steady-state parameters of TcGMPR against GMP and NADPH were characterized by charting the initial velocity values as Lineweaver-Burk plots (Fig. 12). The values of K_m GMP, K_m NADPH, and k_{cat} were determined to be 91.6 ± 4.7 μM, 11.3 ± 2.3 μM, and 0.499 ± 0.014 s^{-1}, respectively. Again, these values were quite similar to the reported values for TbGMPR (Table 3). But more importantly, they were significantly different from those of mammalian enzymes (Bessho *et al.*, 2016). The values of these parameters indicated that TcGMPR has at least 4-fold lower affinity to GMP, but up to 5-fold stronger affinity to NADPH, compared to those of mammalian GMPRs. Moreover, the k_{cat} value of TcGMPR indicated that the

Trypanosomatidae enzyme is up to 1.7-fold more efficient compared to its mammalian counterparts for catalyzing GMP conversion to IMP.

The similarity of the kinetics implied that the inhibitor of TcGMPR might also inhibit TbGMPR, and vice versa. The significant kinetic differences with mammalian GMPR suggested that the development of selective *Trypanosoma* GMPR inhibitors is possible.

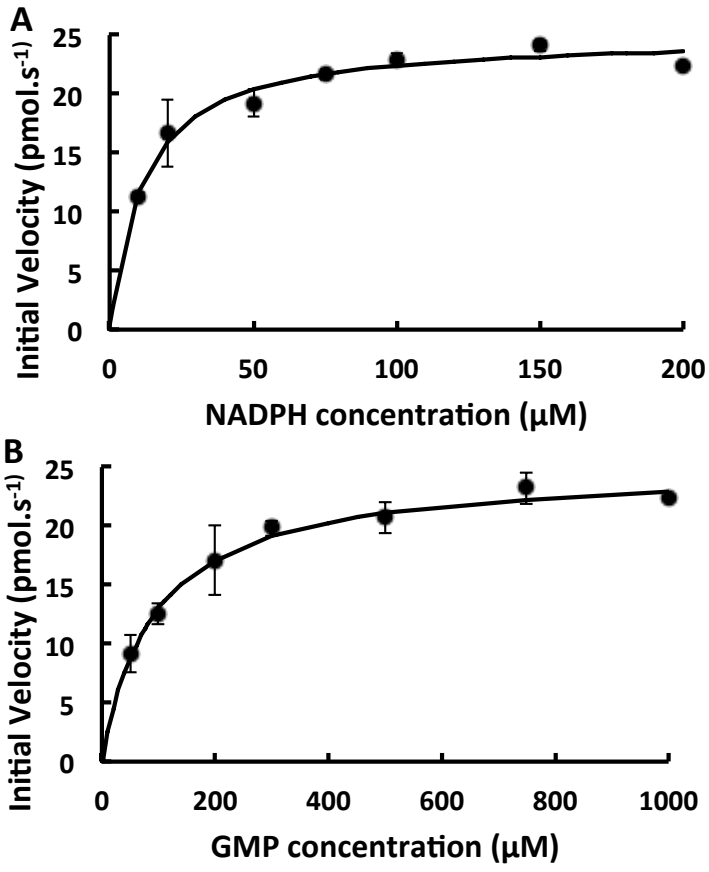


Fig. 12. Steady-state kinetic analysis of TcGMPR

(A) The K_m NADPH was determined at a fixed GMP concentration of 1.0 mM and varying concentration of NADPH. (B) The K_m GMP was determined at a fixed NADPH concentration of 200 μM and varying concentration of GMP. The initial velocity values of the reactions were fitted to the Michaelis-Menten equation using GraFit 7 software. Each point represents mean ± standard deviation from three independent experiments.

Table 3. Comparison of enzymatic parameters of TcGMPR to other GMPR

	k_{cat} (s^{-1})	$K_{m\ GMP}$ (μM)	$K_{m\ NADPH}$ (μM)
TcGMPR[a]	0.499 ± 0.014	91.6 ± 4.7	11.3 ± 2.3
TbGMPR[b]	0.519 ± 0.012	89.3 ± 9.0	12.3 ± 0.8
HsGMPR1[b]	0.284 ± 0.006	22.1 ± 2.2	34.8 ± 4.3
HsGMPR2[b]	0.265 ± 0.016	17.8 ± 3.5	29.3 ± 3.2
BtGMPR1[b]	0.243 ± 0.004	13.5 ± 1.3	54.1 ± 5.0
BtGMPR2[b]	0.296 ± 0.009	22.6 ± 4.2	62.1 ± 7.0

[a]: Activity was measured at 35°C, 75 mM Tris-HCl buffer (pH 7.0), 100 mM KCl, 3 mM EDTA, 1 mM DTT, and 0.1 mg/ml BSA.

[b]: Activity was measured at 35°C, 50 mM sodium phosphate buffer (pH 7.0), 100 mM KCl, 3 mM EDTA, and 1 mM DTT (Bessho *et al.*, 2016).

3.6. Inhibition of TcGMPR by mycophenolic acid

Mycophenolic acid (MPA) (Fig. 13) is a potent inhibitor of mammalian IMPDH. However, since IMPDH and GMPR have similar substrates and primary structure, it is possible that a same inhibitor could inhibit both enzymes. The TcGMPR inhibition assay of MPA showed a clear inhibitory activity with IC_{50} of 239.6 ± 26.7 μM (Fig. 14). MPA also showed a potent inhibition activity in the *T. congolense* culture, where the presence of 1 μM inhibitor resulted in a 99.6% decrease in free-living protozoa (Suganuma *et al.*, 2016). Similar finding on GMPR inhibition by MPA was also reported with *Leishmania major* GMPR, which exerted a K_i value of 20 μM (Smith *et al.*, 2016).

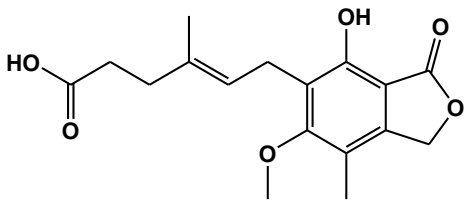


Fig. 13. The structure of mycophenolic acid

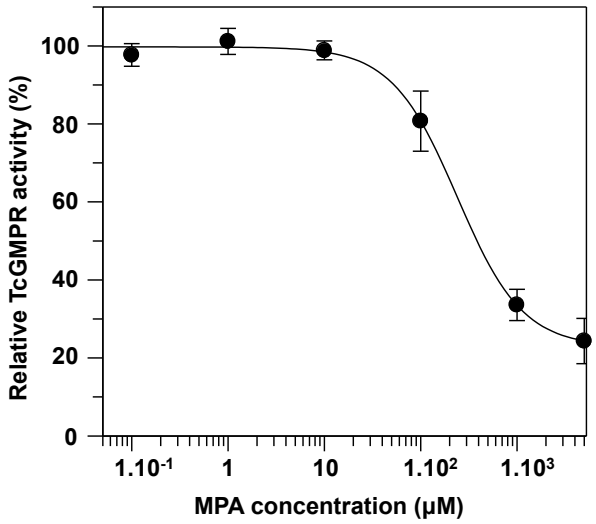


Fig. 14. Inhibitory activity of MPA against TcGMPR

Each data point represents mean ± standard deviation from three independent experiments.

3.7. Activation of TcGMPR by monovalent cation

As stated earlier, primary structure of Kinetoplastide GMPR seemed to resemble IMPDHs more than GMPRs, leading to misannotations of the enzymes. Interestingly, TbGMPR was found to be activated by the presence of cations such as potassium and ammonium, similar to that of IMPDHs (Hedstrom, 2009; Bessho *et al.*, 2016). As a relative of TbGMPR, TcGMPR might show a similar behavior.

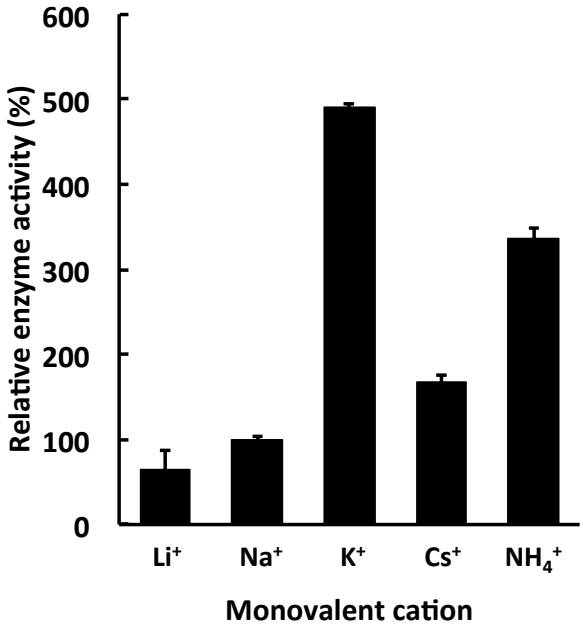


Fig. 15. Effect of monovalent cation on TcGMPR

TcGMPR activity was evaluated in the presence of each monovalent cation in the form of a chloride salt. The activity in the presence of NaCl was set as 100%. Each bar represents mean ± standard deviation from three independent experiments.

The results suggested the positive correlation of cation size to TcGMPR activity. In the presence of smaller cation Li^+ (0.60 Å), the enzyme activity was lowest at 3.8 ± 0.2 nM/s. Subsequently, the addition of larger radius cations: Na^+ (0.95 Å), K^+ (1.33 Å), Cs^+ (1.69 Å), and NH_4^+ (1.48 Å) enhanced the enzyme activity to 5.8 ± 0.2 nM/s, 28.5 ± 1.0 nM/s, 9.7 ± 0.8, and 19.5 ± 2.5 nM/s, respectively (Fig. 15).

A similar activation pattern was also reported in IMPDHs, where the presence of smaller ions such as Li^+ and Na^+ could cause a negative (inhibition), positive (activation), or neutral effect (no effect) on enzyme activity, but larger ions (K^+, Rb^+, Cs^+, Tl^+, and NH_4^+) always activate the reaction (Xiang, Taylor & Markham, 1996; Zhou *et al.*, 1997; Hedstrom, 2009). Mammalian GMPRs on the other hand, showed no activation in the presence of K^+ and NH_4^+ in comparison with Na^+ (Bessho *et al.*, 2016). This finding further characterized the difference between Kinetoplastida and mammalian GMPR.

3.8. Reverse reaction of GMPR

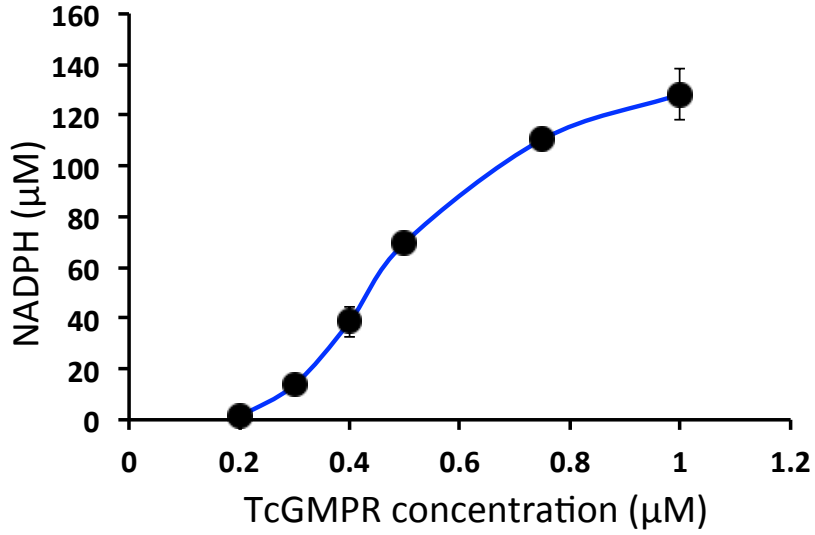


Fig. 16. Reverse reaction of GMPR

TcGMPR was able to convert IMP to GMP in the presence of NH_4^+. Each point was expressed as the mean amount of NADPH formed during reaction ± standard deviation from three independent experiments.

Interestingly, GMPR could also catalyze a reverse reaction: the direct conversion of IMP to GMP. This activity was found to be directly dependent on the concentration of ammonium ion in the reaction (Patton *et al.*, 2011). The opposite reaction by TcGMPR was observed in an enzyme-concentration-dependent manner. However, the specific activity of the reverse reaction was quite low compared to the conventional reaction (Fig. 16). Furthermore, the activation of the deamination reaction could be observed in a much lower ammonium concentration than the progression of the aforementioned reverse reaction. This illustrated the complexity of the role of ammonium ion for GMPR, since it facilitates both forward and reverse reaction.

Nevertheless, the ability of GMPR to catalyze the conversion between GMP and IMP in both directions suggests that the enzyme might have an important role in the early

development of IMPDH/GMPR family, since the earliest forms of life are believed to have emerged in an ammonia rich environment (Zahnle, 2006). *Trypanosome* itself has been known as an ammonotelic organism, and is able to tolerate relatively high ammonium concentrations (Yoshida & Plessmann Camargo, 1978; Zeuthen *et al.*, 2006; Opperdoes & Coombs, 2007). Therefore, the protozoa might be able to survive when there is a high concentration of ammonium ion in the blood and under repressed activity of other enzymes, provided that TcGMPR can produce sufficient GMP for its survival (Patton *et al.*, 2011).

3.9. Identification of BAT33662.1, an TcIL3000_5_1940 orthologue

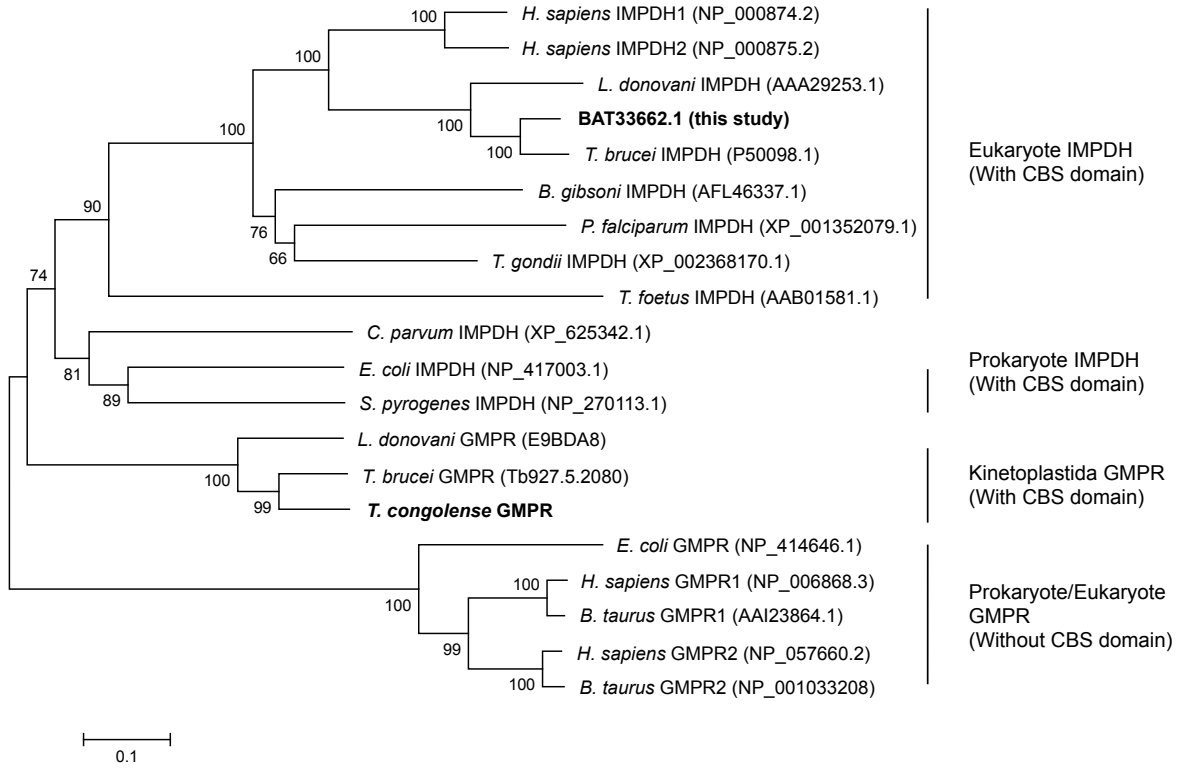


Fig. 17. Phylogenetic tree for BAT33662.1.

After the characterization of TcGMPR, an orthologous gene on *T. congolense* genome was found under accession code of BAT33662.1. We suspected that this enzyme is

a novel IMPDH from *T. congolense*. To confirm, this enzyme was subjected to both IMPDH and GMPR assay solution.

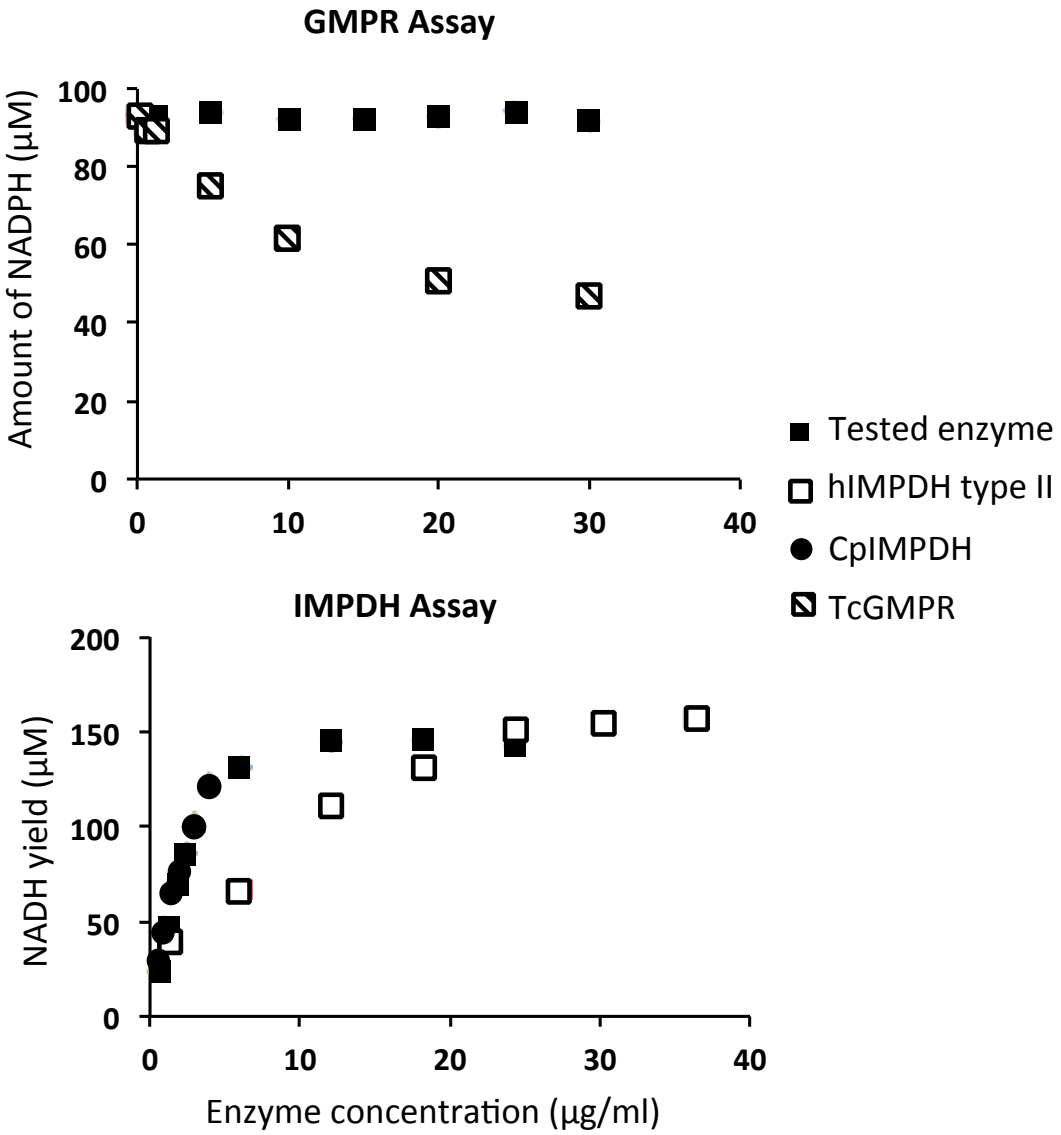


Fig. 18. Enzymatic identification of BAT33662.1

The assay showed clearly that the tested enzyme exerted an IMPDH activity, but not GMPR. Therefore, it was confirmed that the tested enzyme is a novel IMPDH from *T. congolense* (TcIMPDH). The amino acid sequence of the protein is as shown in Fig. 19.

MSNANLRTKTMRDGNTAEELFSHDGLTFNDFIILPGFIDFDASKVNVSGQFTKKILLHLP
LVSSPMDTVTESSMARAMALMGGIGVIHNNCPVAQQAQMVRSVKLYRNGFIMKPKS
VPPTAPVSVIKDINVTKGISGILVTEGGRHDGKLLGIVCSKDIDFVRDDTAPVSQYMTKRK
NMTVERYPIKLEEAMDVLNRSRHGYLPVLNDRDEVMCLCSRRDAVRARDYPNSSLDRN
GHLLCAAATSTRESDKERVAALATAGVDVLVLDSSQGNTIFQVSFIHWVKKTYPHLEVV
AGNVVTQDQAKNLIDAGADALRVGMGSGSICITQEVLACGRPQATAVYKVARYAASR
GVPCIADGGLKNVGDVCKALAIGANVAMLGSMIAGTTEAPGEYFFKDGMRLKGYRGM
GSIDAMLQGRESGKRYLSENENIQVAQGVAGAVLDKGSVLKLLAYVHKGLQQAAQDIG
EVSFGVIREKMYEGQVLFNRRSLTAQSEAAVHSLHHYERKLFASKL

Fig. 19. Amino acid sequence of the novel TcIMPDH

3.10. Inhibition of TcIMPDH by MPA

MPA is a well-known IMPDH inhibitor, and inhibits mammalian IMPDH more strongly than microbial IMPDH (Umejiego *et al.*, 2004; Hedstrom, 2009). Therefore, inhibition of MPA to TcIMPDH was expected.

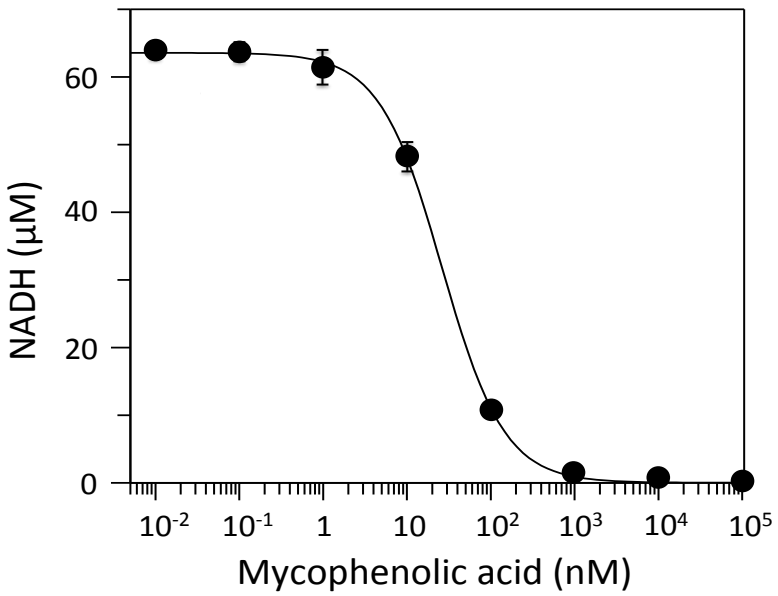


Fig. 20. Inhibitory activity of MPA to TcIMPDH

As shown in Fig. 20, inhibition of TcIMPDH was observed in a dose-dependent manner. The calculated IC_{50} of MPA against TcIMPDH was 26 nM. Compared to the inhibition to TcGMPR, it was clearly shown that MPA more strongly inhibited TcIMPDH, with 4-mangitude lower IC_{50} value.

3.11. A distinction point between GMPR and IMPDH

After the identification of IMPDH and GMPR from *T. congolense*, the author tried to search the main distinction point in the primary structure between IMPDH and GMPR. Previously, some specific amino acid residues have been proposed for this rapid identification of both enzymes. For example, the consensus sequence Tyr303-Arg304 and Glu307 (human GMPR2 numbering) was suggested as the residues that characterize all GMPRs (Hedstrom, 2012). In IMPDHs, the position 303-304 is usually non-conserved and amino acid in position 307 was Gln instead of Glu.

However, this might not be the case because Tyr303-Arg304 dyad is also non-conserved in the reported *L. donovani* and *T. brucei* GMPR, while Glu431 (*Tritrichomonas foetus* IMPDH numbering) is also present in several IMPDHs instead of Gln.

However, we found that all GMPRs in this study are conserved residue Leu217-Ser218 of the catalytic loop region (Fig. 21). This conserved dyad lies in a close proximity from the catalytic cysteine. This indicated that the dyad of GMPR might determine the affinity to XMP rather than to IMP. Nevertheless, further enzymatic experiments are needed to verify this finding.

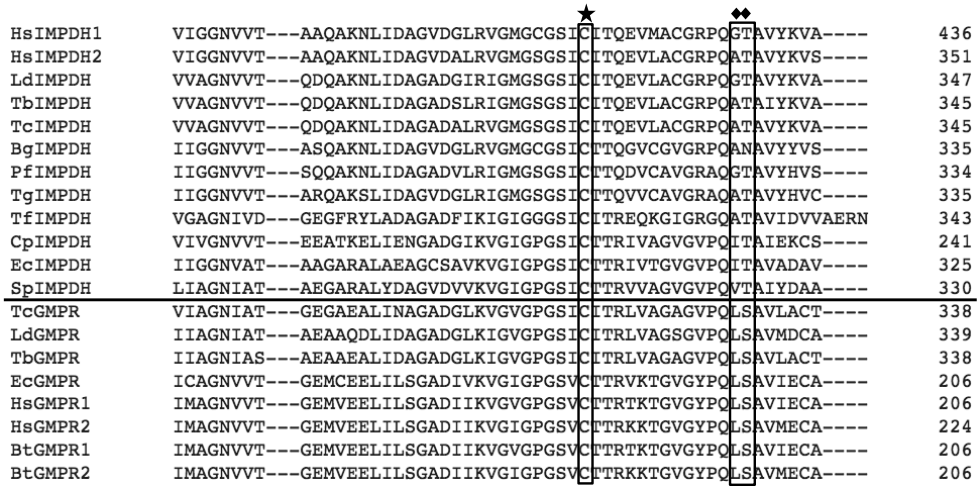


Fig. 21. The distinction point between GMPRs and IMPDHs

The amino acid sequences of the active loop of GMPRs and IMPDHs were aligned. Diamond symbols indicate Leu217-Ser218 (HsGMPR2 numbering), the conserved residues of GMPRs. Star symbol indicates Cys204, an important catalytic residue for both GMPR and IMPDH.

Amino acid sequence was taken from NCBI database unless stated otherwise. Protein sequences for *H. sapiens* (accession number of HsIMPDH1: NP_000874.2, HsIMPDH2: NP_000875.2, HsGMPR1: NP_006868.3, HsGMPR2: NP_057660.2), *B. taurus* (BtGMPR1: AAI23864.1 [Uniprot], BtGMPR2: NP_001033208), *L. donovani* (LdIMPDH: AAA29253.1 [Uniprot], LdGMPR: E9BDA8 [Uniprot]), *T. brucei* (TbIMPDH: P50098.1 [Uniprot], TbGMPR: Tb927.5.2080 [TriTrypDB]), ***T. congolense* (TcIMPDH: BAT33662.1 [Uniprot], TcGMPR: TcIL3000_5_1940 [TriTrypDB])**, *B. gibsoni* (BgIMPDH: AFL46337.1), *P. falciparum* (PfIMPDH: XP_001352079.1), *T. gondii* (TgIMPDH: XP_002368170.1), *T. foetus* (TfIMPDH: AAB01581.1 [Uniprot]), *C. parvum* (CpIMPDH: XP_625342.1), *E. coli* (EcIMPDH: NP_417003.1, EcGMPR: NP_414646.1), and *S. pyrogenes* (SpIMPDH: NP_270113.1) were aligned using ClustalW program.

4. CONCLUSION

In conclusion, the present study revealed that TcIL3000_5_1940 is a GMPR-encoded gene of *T. congolense*. TcGMPR showed remarkably similar kinetic parameters to TbGMPR, and they differed significantly to mammalian GMPRs. In addition, Leu217-Ser218 dyad was identified by the amino acid alignment as a practical distinction point to identify GMPRs from IMPDHs. Lastly, a selective IMPDH inhibitor, mycophenolic acid, was found to inhibit TcGMPR activity, demonstrating its potential as a lead compound for the development of dual-target chemotherapeutic agents against *Trypanosoma* infection.

Additionally, a protein encoded by BAT33662.1 was identified as an IMPDH from *T. congolense*. Further kinetic study of this enzyme will be performed in the future.

CHAPTER III. HIGH THROUGHPUT SCREENING FOR IMPDH INHIBITORS

1. INTRODUCTION

1.1. The role of IMPDH in various diseases

As mentioned earlier, IMPDH is one of the enzymes involved in the purine nucleotide biosynthesis. It catalyzes the conversion of IMP to XMP, which will eventually be converted to GMP for nucleic acid biosynthesis. Inhibition of IMPDH has been proposed as a therapeutic strategy for various purposes, such as the treatment of degenerative and infectious diseases (Franchetti & Grifantini, 1999; Ratcliffe, 2006; Hedstrom, 2009; Mitsuhashi *et al.*, 2010; Suganuma *et al.*, 2016; Pua *et al.*, 2017; Tong *et al.*, 2018). Therefore, the discovery of IMPDH inhibitors is highly beneficial.

1.2. The significance of human IMPDH

IMPDH in human consists of two isoforms, type I and type II (hIMPDH I and II). While hIMPDH I constantly expressed at a low level in various tissues and contribute in maintaining homeostasis, hIMPDH II has been found to expressed mainly in rapidly replicating cells. This renders hIMPDH II as a drug target for various puposes, such as suppressing the replication of cancer cells, lymphocytes, and virus. Therefore, the discovery of hIMPDH II inhibitors is necessary.

1.3. The significance of *Cryptosporidium parvum* IMPDH

Cryptosporidium parvum is a waterborne pathogen, which causes watery or mucoid diarrhea and abdominal pain in many mammal species, including human. The infection is usually self-limiting in immunocompetent patients. Unfortunately, the infections could be severe in immunocompromised patients, such as children, elderly person, or AIDS patients (DuPont *et al.*, 1995; Hunter & Nichols, 2002; Fayer, 2004).

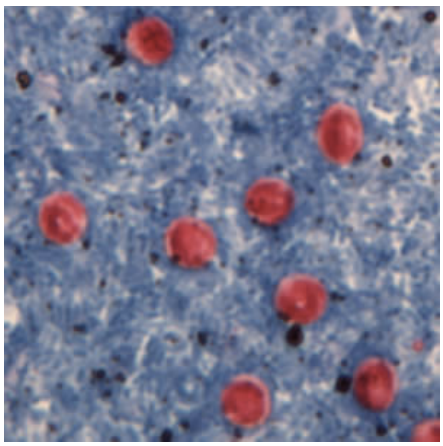


Fig. 22. *Cryptosporidium parvum* oocyst with Ziehl-Neelson staining (CDC, 2017)

Cryptosporidiosis reached its prominence since the Milwaukee massive outbreak in spring 1993, in which up to 403,000 residents were infected with the pathogen. Other smaller cases of infection have also been reported in North America, United Kingdom, and Japan between 1984 and 1999 (Mac Kenzie *et al.*, 1994; Fayer, Morgan & Upton, 2000; Fayer, 2004).

Current chemotherapeutic agent for cryptosporidiosis includes nitazoxanide, paromomycin, and azithromycin. These drugs successfully reduced symptomatic manifestations and lower oocyst shedding in crypstosporidiosis patients. Nonetheless, the clinical outcomes were significantly varied between one patient and other patients (Mead, 2002; Gargala G, 2008).

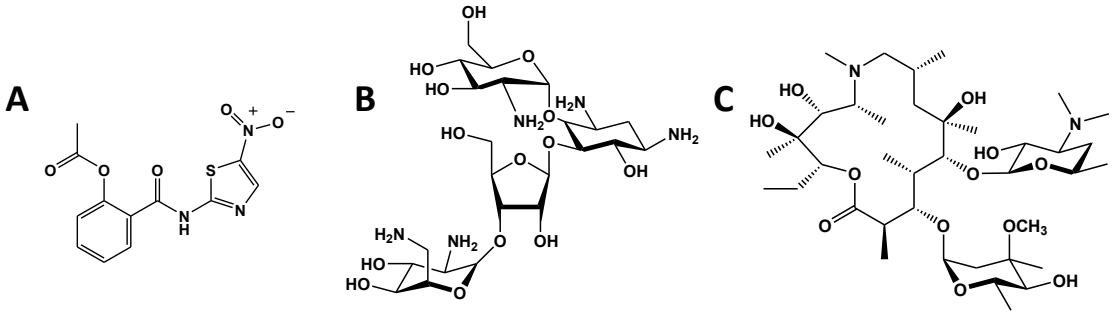


Fig. 23. Chemotherapeutic agents for cryptosporidiosis

(A) Nitazozanide, (B) Paromomycin, and (C) Azithromycin

In the last decade, the IMPDH of *C. parvum* was found to play an essential role in guanine nucleotide production in *C. parvum*. Several studies have proven that the inhibition of the enzyme could effectively disrupt the nucleic acid synthesis in the protozoa. Therefore, this enzyme is considered as a chemotherapeutic target against *C. parvum* infection.

1.4. High Throughput Screening

High Throughput Screening (HTS) is an experimentation method, which involves an assay of a large numbers of chemicals (often referred as chemical libraries), against certain biological targets. This system has been applied for various purposes, from the study of enzyme-inhibitor interaction until the elucidation of biosynthesis pathways. One integral part of this system is the automated or semi-automated solution handling and high sensitivity detection system (Liu, Li & Hu, 2004). This mechanization provides scientists with the capability to carry out more bioassays in shorter time.

The value of HTS system has been demonstrated by its outcomes, such as the discovery of anti-rheumatic auranofin and coronary dilator benzbromarone as novel inhibitors of *Candida albicans* biofilm formation, anti-histamin zolantidine as an anti-

malarial agent, and antineoplastic agent mitoxantrone as a metallo-*β*-lactamase inhibitor (Minond *et al.*, 2009; Lucumi *et al.*, 2010; Siles *et al.*, 2013).

1.5. High Throughput Screening of IMPDH inhibitors

Previously, several high-throughput studies has been conducted to screen IMPDH inhibitors (Umejiego *et al.*, 2008; Dunkern *et al.*, 2012; Cox *et al.*, 2016). However, some limitations were present in the assays: (1) the measurements of IMPDH activity were by OD_{340} or fluorescence, thus prone to false negative detections, (2) the assays were conducted with a relatively high amount of enzyme, and (3) there was no report of the repurposing of known compounds.

This study aimed to discuss the discovery and the characterization of IMPDH inhibitors discovered from a bioluminescence-based high-throughput screening of 3,200 compounds (Fig. 24). Half of the compounds were known compounds, and the other half are novel compounds synthesized by the Faculty of Pharmacy, Hokkaido University. The compounds that identified as “hit” inhibitors were then subjected into inhibition kinetic study against *C. parvum* IMPDH (CpIMPDH) and human IMPDH type II (hIMPDH II). Overall, this study offered a new perspective of available classes of IMPDH irreversible inhibitor, providing a broad range of lead compounds for the development of more potent IMPDH inhibitors (Cuny, Suebsuwong & Ray, 2017).

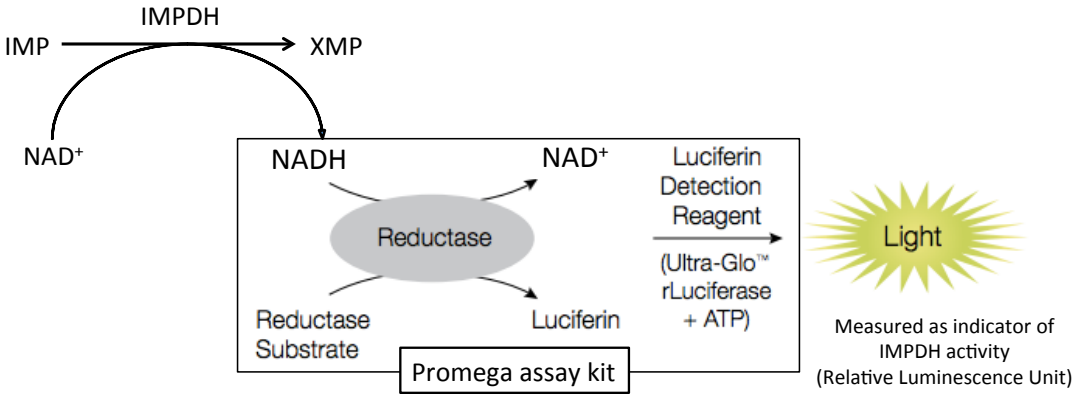


Fig. 24. Luminescence detection of IMPDH activity

2. MATERIAL AND METHODS

2.1. Molecular methods

The coding sequence of CpIMPDH was amplified by PCR using primer sets 5'-TTTTGGATCCTCAAACATGGGTACA-3' and 5'-TTTTGAATTCCTATTTACT-ATAATT-3'. The PCR product was cloned into pCR2.1-TOPO vector (Invitrogen Japan KK, Tokyo, Japan), and the complete gene sequence was confirmed using ABI PRISM 3100 Genetic Analyzer (Applied Biosystems, Tokyo, Japan). CpIMPDH gene was digested by *Bam*HI and *Eco*RI, and the digested gene was inserted into a pGEX-6P-2 plasmid (GE Healthcare Bio-Science Corp., UK). The plasmid was then transformed to ECOS *E. coli* BL21 (DE3) (Wako Pure Chemical Ind., Ltd., Japan).

hIMPDH II plasmid was a generous gift from Prof. Lizbeth Hedstrom, Brandeis University, USA. The plasmid was transformed in the same manner as CpIMPDH.

2.2. Expression and purification of recombinant IMPDH

Cells carrying previously described plasmids were grown overnight at 30°C in 50 ml 2xYT broth containing 100 μg/ml ampicillin. Afterwards, the broth was subcultured to 700 ml of medium containing a final concentration of 1 mM isopropyl-1-thio-*β*-galactopyranoside (Sigma-Aldrich Japan, Tokyo, Japan) and 100 μg/ml ampicillin. After 5 h incubation at 25°C, cells were harvested by centrifugation, washed with PBS solution, and stored frozen at −80°C until usage.

2.3. Determination of enzyme kinetic parameter of CpIMPDH and hIMPDH II

Both enzymes were subjected to IMPDH assay solution containing 100 mM KCl, 3 mM EDTA, 1 mM DTT, and 0.1 mg/ml BSA in 50 mM Tris pH 8.0 (25°C). For CpIMPDH, in the kinetic measurement against NAD^+, IMP concentration was kept

constant at 250 μM. While in kinetic measurement against IMP, NAD^+ concentration was kept constant at 500 μM. As for hIMPDH II, in the kinetic measurement against NAD^+, IMP concentration was kept constant at 250 μM. While in kinetic measurement against IMP, NAD^+ concentration was kept constant at 100 μM. Initial velocity against IMP was fitted into Michaelis-Menten equation (Eq. 1). Initial velocity against NAD^+ was fitted into uncompetitive substrate inhibition equation (Eq. 2).

$$v = \frac{V_{\mathrm{m}}[\mathrm{S}]}{(K_{\mathrm{m}}+[S])} \qquad \text{(Equation 1)}$$

$$v = \frac{V_{\mathrm{m}}}{\left(1+\frac{K_{\mathrm{m}}}{[\mathrm{S}]}+\frac{[\mathrm{S}]}{K_{\mathrm{ii}}}\right)} \qquad \text{(Equation 2)}$$

where v is reaction velocity, Vm is the maximal velocity, [S] is substrate concentration, K_{m} is the Michaelis-Menten constant for the substrate, and K_{ii} is the intercept inhibition constant.

Plot fitting of inhibitory study was carried out using GraphPad Prism 7.0 (GraphPad Software, San Diego, USA).

2.4. High-Throughput Screening of IMPDH inhibitors

The HTS assay was established using NAD(P)H-Glo Assay Kit (Promega, Madison, WI, USA). Briefly, 10 μl of substrate solution containing 50 mM Tris-HCl pH 8.0, 200 mM KCl, 0.1 mg/ml BSA, 1.6 mM β-NAD^+ (Oriental Yeast Co., Tokyo, Japan), 100 μM IMP (Sigma-Aldrich Japan, Tokyo, Japan), and the assay kit was added to white 384-well plates. Mycophenolic acid (APAC Pharmaceutical LLC, Hangzhou, China), a known IMPDH inhibitor, or chemical library compounds were also added to the wells in concentration of 10 μM. Reaction was started by addition of 10 μl enzyme solution containing 50 mM Tris-HCl pH 8.0, 0.1 mg/ml BSA, and CpIMPDH. Reaction was carried out at 30°C for 30 minutes in dark. Solution handlings was carried out using Mosquito LCP (TTP LabTech Ltd., Melbourn, UK) and Multidrop Combi (Thermo

Scientific, Waltham, MA, USA). The production of NADH was monitored by the measurement of luminescence (RLU) using either VERITAS Microplate Luminometer (Turner Biosystems, Sunnyvale, CA, USA) or EnSpire Multimode Reader (Perkin-Elmer, Waltham, MA, USA).

The counter assay was carried out by directly incubating assay kit, the library compounds, and appropriate amount of NADH. The produced luminescence was monitored.

IC_{50} values were calculated by plotting the recorded NADH yield against log of compound concentration in GraFit ver. 7 (Erithacus Software, UK). All screening assays in this study was conducted with 0.5% DMSO as vehicle and library compound concentration of 10 μM unless stated otherwise.

2.5. Dialysis for determination of inhibition reversibility

CpIMPDH (0.6 μM) was incubated with inhibitor compounds (500 μM) or vehicle (DMSO 0.5%) for 1 hour at room temperature. The mixture solution (0.3 ml) was then dialyzed overnight with 2-times 45 ml Tris-HCl buffer pH 8.0 at 4°C. The concentration of protein in the dialyzed solution was determined by Bradford assay. The residual IMPDH activity was then evaluated by monitoring the time-course reaction of the enzyme.

2.6. Kinetics of IMPDH inhibition by hit compounds

2.6.1. Irreversible inhibition

Standard IMPDH assay solution contained 50 mM Tris-HCl pH 8.0, 100 mM KCl, 3 mM EDTA, 0.1 mg/ml BSA, and an appropriate amount of inhibitor with a total volume of 270 μl. Substrate concentrations in the solution were 500 μM NAD^+ and 250 μM IMP for CpIMPDH, 100 μM NAD^+ and 250 μM IMP for hIMPDH II. Reaction was started by the addition of 30 μl enzyme solution. The activity of the enzyme was measured by

monitoring NADH production in either absorbance at 340 nm or fluorescence emissions at 465 nm.

The exponential inactivation was quantified by fitting the decay progress curve to Eq. 3 (Morrison & Walsh, 2006; Baici, 2013):

$$R_t - R_0 = \frac{V_0}{k_{\text{obs}}}(1 - e^{-k_{\text{obs}}.t}) \qquad \text{(Equation 3)}$$

where R_t is the absorbance (OD_{340}) or fluorescence at time t, R_0 is the initial absorbance or fluorescence at time 0, V_0 is the initial reaction rate, and k_{obs} is the observed rate constant of enzyme inactivation. Acquired k_{obs} values then fitted into Eq. 4 to obtain k_{on} value:

$$k_{\text{obs}} = \frac{k_{\text{on}}\,[\text{I}]}{1+\frac{[\text{S}]}{K_{\text{m}}}} \qquad \text{(Equation 4)}$$

where k_{on} is the apparent second-order rate constant for IMPDH inactivation, [I] is inhibitor concentration, [S] is IMP concentration, and K_m is Michaelis-Menten constant for IMP.

Plot fitting of inhibitory study was carried out using GraphPad Prism 7.0 (GraphPad Software, San Diego, USA). Values of inhibitory activity are mean ± SD for two independent experiments.

2.6.2. Reversible inhibition

Reversible inhibition parameter was measured by monitoring the formation of NADH in various substrate concentrations in the presence and absence of inhibitor. Assay was carried out with standard IMPDH assay solution as mentioned in 2.4.1. Data were fitted into noncompetitive inhibition (Eq. 5) or mixed model inhibition (Eq. 6):

$$v = \frac{V_{\text{m}}[S]}{\left(K_{\text{m}}\left(1+\frac{[\text{I}\}}{K_{\text{i}}}\right)+[S]\left(1+\frac{[\text{I}]}{K_{\text{i}}}\right)\right)} \qquad \text{(Equation 5)}$$

$$v = \frac{V_{\mathrm{m}}[\mathrm{S}]}{\left(K_{\mathrm{m}}\left(1+\frac{[\mathrm{I}]}{K_{\mathrm{is}}}\right)+[S]\left(1+\frac{[\mathrm{I}]}{K_{\mathrm{ii}}}\right)\right)} \qquad \text{(Equation 6)}$$

where v is reaction velocity, V_{m} is the maximal velocity, [S] is substrate concentration, K_{m} is the Michaelis-Menten constant for the substrate, K_{i} is inhibition constant when the inhibitor shows equal affinity to free enzyme and enzyme-substrate complex, K_{is} is the slope inhibition constant, and K_{ii} is the intercept inhibition constant.

Plot fitting of inhibitory study was carried out using GraphPad Prism 7.0 (GraphPad Software, San Diego, USA). Values of inhibitory activity are mean ± SD for two independent experiments.

2.7. Molecular docking of IMPDH inhibitors

2.7.1. Preparation of small molecule ligands

Structures of hit compounds were prepared with SPARTAN ‘16 (Wavefunction, Inc., Irvine, CA, USA). Briefly, molecules were constructed and optimized with Molecular Mechanics MMFF mode. Twenty conformers with the lowest energy were selected for next optimizations. Next, the energy of the conformers was calculated by Density Functional ωB97X-D, 6-31G* mode. Ten conformers with the lowest energy were selected. Lastly, the conformers were subjected to Equilibrium Geometry, Semi-Empirical PM3 mode, and the conformer with the lowest energy was saved for further experiment.

2.7.2. Preparation of protein

The x-ray crystal of hIMPDH II protein model (accession code: 1NFB) was prepared with BIOVIA Discovery Studio 2017 R2 (Dassault Systemes Biovia Corp., San Diego, CA, USA) and AutoDock Tools (The Scripps Research Institute, La Jolla, CA, USA). Chain A of the dimer protein was used for the experiment. Water molecule and ligands were deleted, and polar hydrogen was added.

2.7.3. Molecular docking

Molecular docking was performed with Autodock Vina (The Scripps Research Institute, La Jolla, CA, USA). Docking configuration was set as follows to include both binding sites of IMPDH:

center_x: 87.962

center_y: 46.668

center_z: 4.916

size_x: 38

size_y: 28

size_z: 36

Exhaustiveness: 50

Binding models that showed rational protein-ligand interaction was selected. Result visualization was generated with PyMOL (Schrödinger, LLC) and LigPlus (EMBL-EBI, Cambridge, UK).

3. RESULTS AND DISCUSSION

3.1. Analysis of CpIMPDH and hIMPDH II isolates

The kinetic parameters of IMPDH isolates were measured to ensure the comparability with previously reported enzymes. The kinetic parameters of both enzyme isolates were found to be comparable with the previously reported isolates (Fig. 24, 25, Table 4, 5). Therefore, both enzymes were valid to be used in the further study.

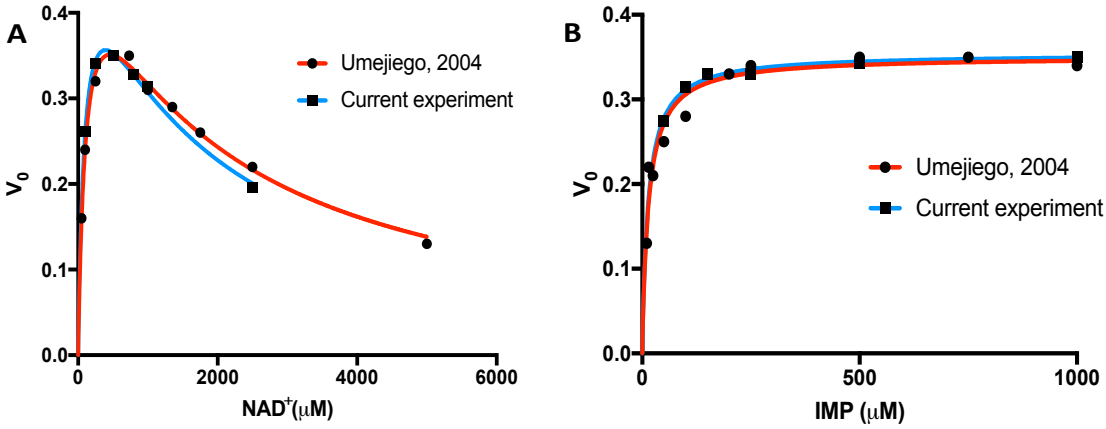


Fig. 25. Kinetic determination of CpIMPDH

The kinetics of CpIMPDH isolate were compared to a previous report (Umejiego *et al.*, 2004). (A) Kinetics against NAD^+, IMP concentration was kept constant at 250 μM. (B) Kinetics against IMP, NAD^+ concentration was kept constant at 500 μM. Initial velocity (V_0) are in arbitrary units. V_0 values against IMP were fitted into Eq. 1, against NAD^+ into Eq. 2.

Table 4. Kinetics of CpIMPDH

	Umejiego, 2004	Current experiment
K_m NAD (μM)	118.9	103.0
K_{ii} NAD (μM)	1,765.0	1,501.0
K_m IMP (μM)	14.6	13.7

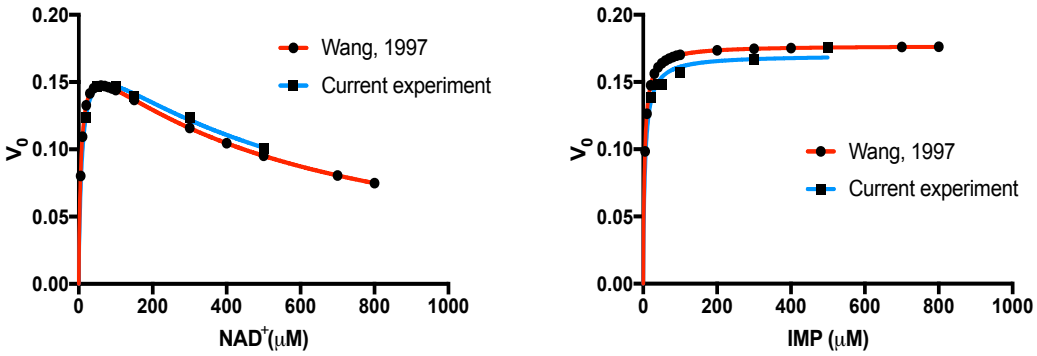


Fig. 26. Kinetic determination of hIMPDH II

The kinetics of hIMPDH II isolate were compared to a previous report (Wang & Hedstrom, 1997). (A) Kinetics against NAD^+, IMP concentration was kept constant at 250 μM. (B) Kinetics against IMP, NAD^+ concentration was kept constant at 100 μM. V_0 values against IMP were fited into Eq. 1, against NAD^+ into Eq. 2.

Table 5. Kinetics of hIMPDH II

	Wang, 1997	Current experiment
K_m NAD (μM)	6	8.9
K_i NAD (μM)	590	632.3
K_m IMP (μM)	4	5.4

3.2. HTS of chemical library compounds

The chemiluminescence-based HTS system enables assays to be carried out with a low microliter volume but still produce robust and selective signal. The developed system has a Z'-factor value of 0.7, indicating an excellent assay system for screening (Appendix Fig. S1) (Zhang, Chung & Oldenburg, 1999; Sarwono, 2015). CpIMPDH was used for all the screening process.

3.2.1. The first screening

First screening was conducted to screen compounds from the chemical library. In total, 3,200 compounds were screened, comprised of 1,600 novel synthesized compounds of Hokkaido University and 1,600 known bioactive compound.

The screening was conducted on ten 384-well white plates, with 320 compounds tested in each plate. As negative and positive controls, DMSO and MPA were added on both ends of the plates, respectively (Fig. 27).

On the screening, some technical errors occurred. As a result, 200 compound from the known compound library and 340 compounds from the synthetic compound library were excluded from this study. Therefore, only 2,660 compounds were analyzed (Fig. 28). This error might be resulted from a defect of Multidrop Combi machine needle, since majority of the error (row G and H of the plate) was pipetted by the same needle.

Subsequently, the "hit" determination was performed from the remaining compounds based on their RLU values. Compounds that produced RLU value lower than 3-times of standard deviation of negative control (DMSO) were considered a "hit" from the screening. From the first screening, a total of 79 compounds were selected as "hits".

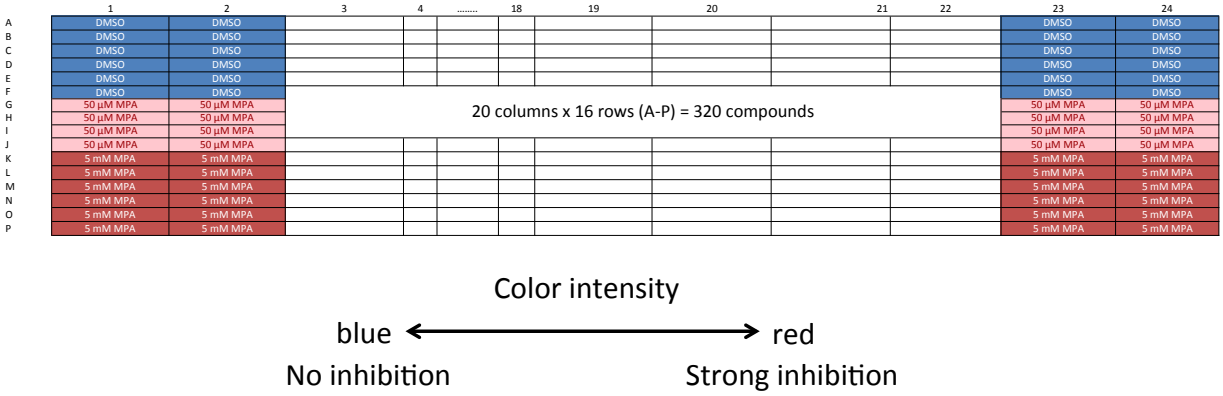


Fig. 27. Scheme of assay plates in the first screening

In each 384-well plate, 320 library compounds were tested. Negative control (DMSO/vehicle) and positive control (MPA in concentration of 50 µl and 5 mM) were added to column 1, 2, 23, and 24 of the plates. Color intensity was used to represent detected luminescent (RLU). Negative control showed no IMPDH inhibition, yielded high RLU from high NADH concentration, depicted as intense blue. In contrast, positive control showed potent IMPDH inhibition, yielded low RLU from low NADH concentration, depicted as intense red. Partial inhibitions were colored in the spectrum between the two controls.

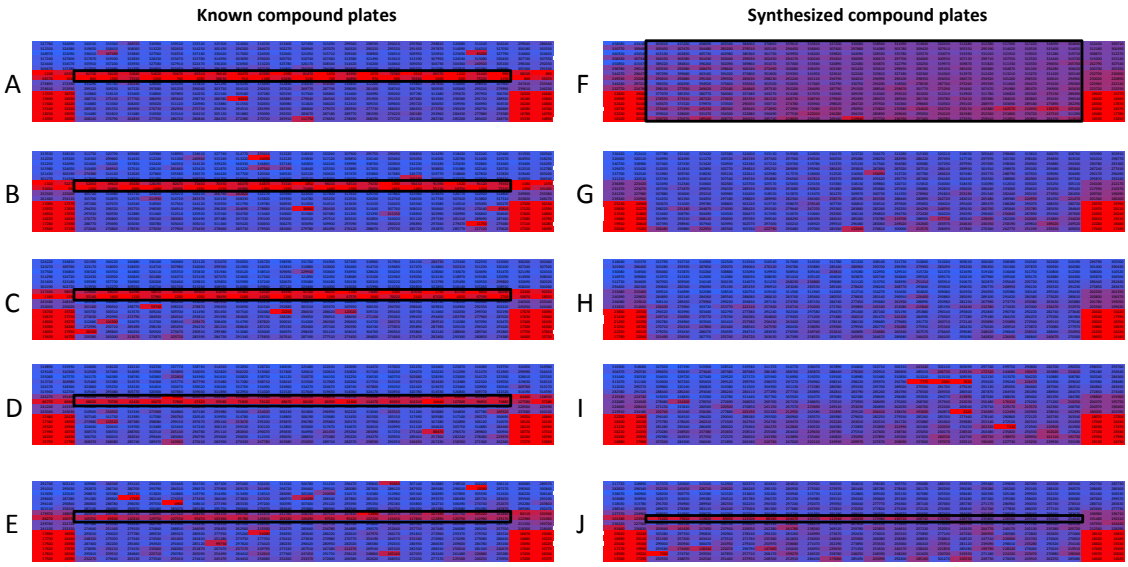


Fig. 28. Heatmap of the first screening

The 10 screening plates for screening of 3,200 library compounds. Known compound library were assayed in plate A-E, while synthesized compounds were assayed in plate F-J. Forty compounds of each plate A-E, all compounds in plate F, and 20 compounds from plate J were disqualified from the study. Disqualified wells were marked by black boxes. Blue represents high NADH concentration, red represent low NADH concentration.

3.2.2. Reproducibility assay

To exclude false positives from the 79 hits in the first screening, reproducibility assay was performed. In this assay, each compound was tested with three replications. From the known compound library, inhibition from 32 compounds was found to be reproducible, and from the synthesized library 19 compounds (Fig. 29).



Fig. 29. Reproducibility assay of hit compounds.

(A) Heatmap of reproducibility assay of 36 hits from known compound library. (B) 32 out of 36 compounds were found to be reproducible. (C) Heatmap of reproducibility assay of 44 hits from synthesized compound library. (D) 19 out of 44 compounds were found to be reproducible.

3.2.3. Dose-dependency assay

Inhibition of a certain compounds to an enzyme is not always a result of stoichiometric enzyme-inhibitor interaction. Some references have shown that some compounds might form a micelle and act as detergent-like inhibitor to the enzyme (Feng *et al.*, 2007). This kind of compound usually shows weak or very steep dose-dependency inhibition. The inhibitory activity of each compound was measured in a 5-points of increasing concentration, with the highest concentration of 50 μM. The 32 compounds

from the known library and 19 compounds from the synthesized library were subjected to this assay.

In addition to these 51 compounds, another nine compounds were also added to the reproducibility assay. These nine compounds are analogues of the 19 synthesized compounds. These additional compounds were expected to provide more insight into the structure-activity-relationship in later phase of this study.

In total, 60 compounds were tested in this stage. All of the compounds were found to display a dose-dependent inhibition. Twenty-nine compounds were found to inhibit in the dose-dependent manner with IC_{50} values less than 10 μM (Fig. 30).

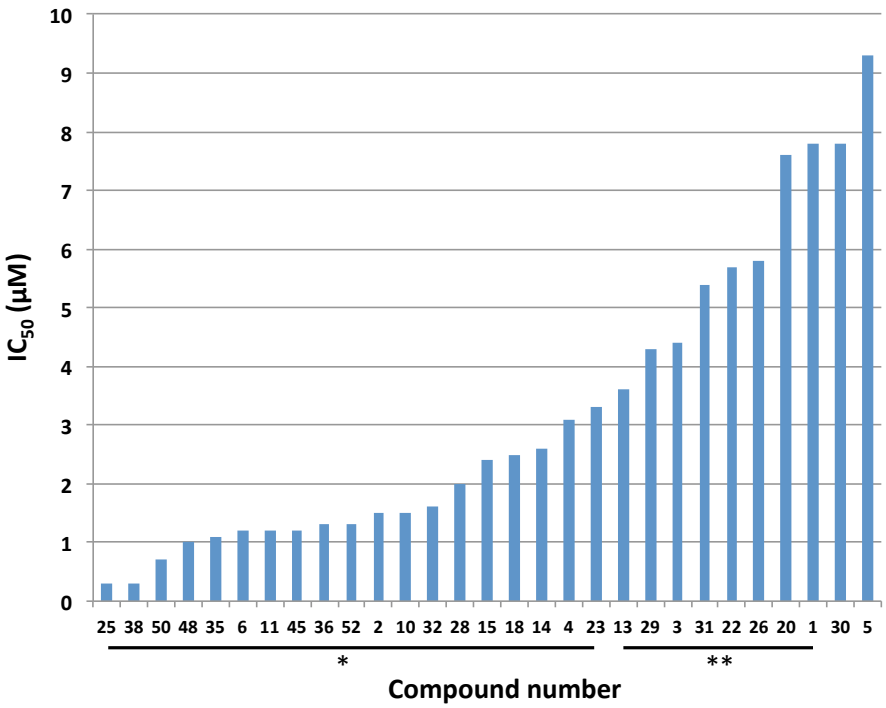


Fig. 30. The twenty-nine compounds with IC_{50} less than 10 μM.

Known compounds were numbered **1-32**, synthesized compounds were numbered **33-60**.

*: 2 asymptotes in dose-dependency assay, **: 1 asymptote and inhibit completely at concentration of 50 μM.

3.2.4. The second screening: Counter assay

All previous assays were performed with luciferase-based assay kit to monitor the formation of NADH (Fig. 24). In principle, the luminescence produced by luciferase was measured as a parameter of IMPDH activity. In the assay kit, two enzymes are necesarry to produce chemiluminescence from NADH: reductase and luciferase. Therefore, it is also possible that the compounds were inhibiting the luciferase or reductase instead of IMPDH. The aim of the counter assay experiment was to exclude compounds that inhibit the assay-kit reaction instead of IMPDH reaction. In this assay, the author compared the difference of recorded luminescence between CpIMPDH-produced NADH reaction (HTS assay) and manually-added standard NADH reaction (assay kit only). The desired inhibitor is an inhibitor that produces decreased luminescence for CpIMPDH-produced NADH but not in manually-added NADH. Sixty compounds from the previous screening were subjected into this stage.

There are two approaches used to address this:

A. Inter-relation model

This model allows simple visualization of the compared conditions. Compounds that showed more than 90% inhibition for CpIMPDH-produced NADH and less than 50% inhibition for manually-added NADH were considered to bean IMPDH inhibitor (Fig. 31).

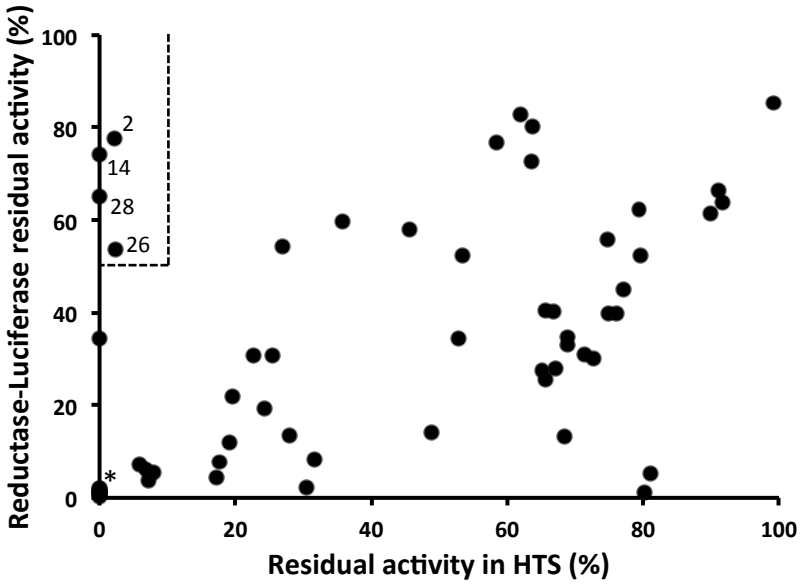


Fig. 31. Inter-relation model of counter assay

The counter assay was performed on 60 compounds to exclude reductase-luciferase inhibitors from hit compounds. Dashed line showed the selection criteria, which eliminated inhibitors that inhibit less than 90% of control IMPDH activity, and more than 50% of control reductase-luciferase activity in the concentration of 10 μM. Four compounds were selected: compound number **2**, **14**, **26**, and **28**. *: A cluster of compounds from synthesized library, which is discussed later in section 3.2.5.

B. Synergistic model

Synergistic model analyzes the same data differently. The postulate is that the recorded inhibition in the HTS assay was the cumulative inhibition between IMPDH inhibition and reductase-luciferase inhibition. Therefore, by subtracting the residual activity in HTS by the residual activity in only assay kit, the inhibition of IMPDH could roughly be estimated.

% inhibition in HTS assay = % inhibition of only assay kit +

% “estimated” inhibition of IMPDH

From this simple calculation, some compounds were found to have more dominant IMPDH inhibition rather than luciferase-reductase inhibition (Fig. 32).

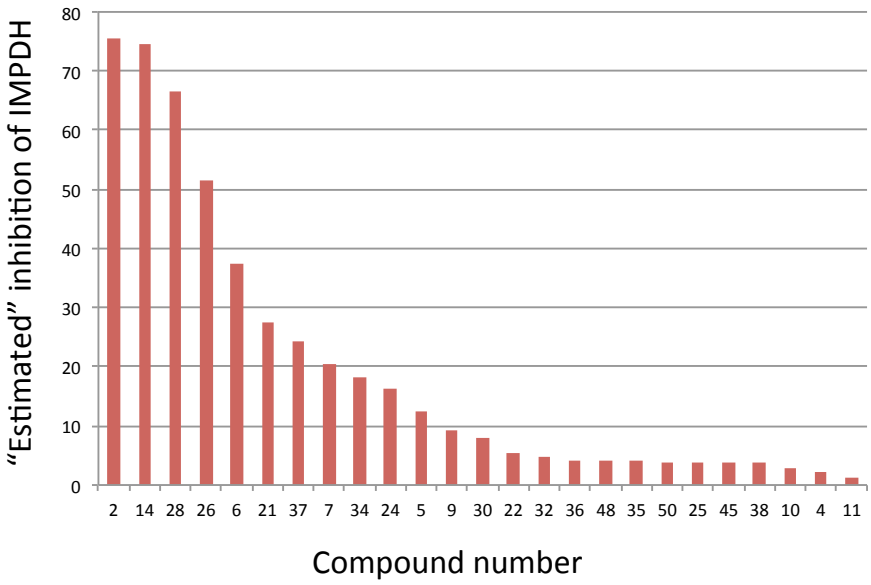


Fig. 32. Synergistic model of counter assay

3.2.5. Final hit compounds

The compounds that showed selectivity to IMPDH in both models were prioritized for the study: disulfiram (**2**), thiram (**14**), ebselen (**26**), and bronopol (**28**). All of these compounds are from the known compound library. In contrast, the novel compounds were found to have relatively low inhibition specificity between IMPDH and reductase-luciferase. Therefore, the selection was conducted based on the IC_{50} value alone: compound **35**, **36** (a replication of compound **45**), **38**, and **48** (a replication of compound **50**) (Fig. 32). These synthesized compounds inhibit both IMPDH and reductase-luciferase (Fig. 31, * symbol)

In the subsequent toxicology analysis, thiram (**14**) were removed from the hit list due to toxicology concerns(Cereser *et al.*, 2001). Compound **38** from synthesized library was currently unavailable for further assays. Therefore, further study was conducted for

compounds **2**, **26**, and **28** from the known compound library, and compounds **35**, **36**, and **48** from the synthesized compound library.

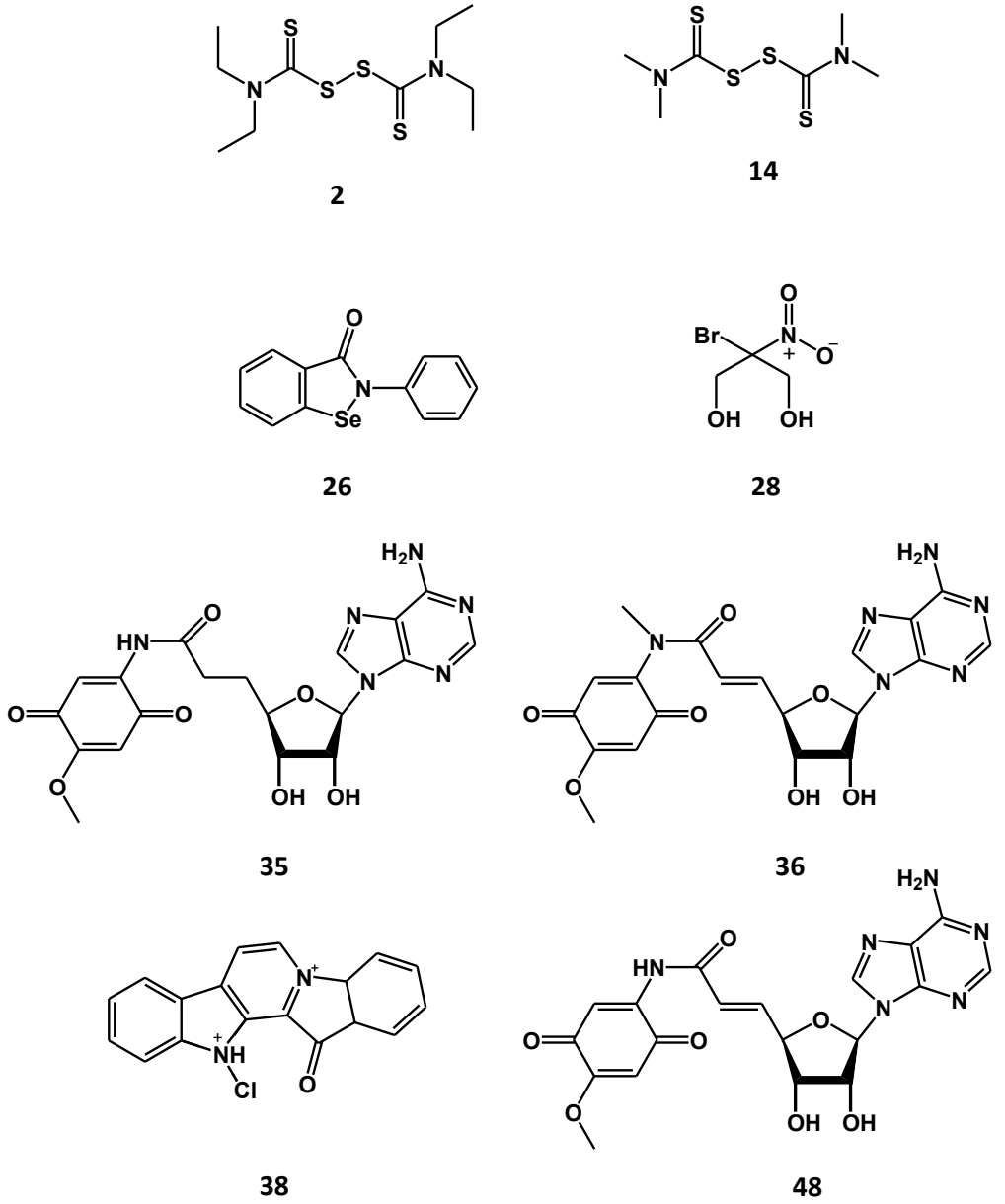


Fig. 33. The structures of the hit compounds

3.3. Analysis of the hit compounds

3.3.1. Measurement of IC_{50} values against CpIMPDH and hIMPDH

The inhibitory activities were then evaluated by directly measuring the formation of NADH by OD_{340} (without assay kit). The principal difference of assay solution

composition between assay with direct measurement of NADH and assay with reductase-luciferase was in the usage of reducing agents. In assays with reductase-luciferase detection system, reducing agents were not used due to the possibility of interfering with the detection system. However, for enzymes that require cysteine as a catalytic residue, reducing agents such as DTT or glutathione are commonly added to the assay solution to protect the residue from reactive inactivator.

Upon IC_{50} measurement in the presence of DTT as reducing agent, a significant decrease of inhibitory activity was observed for bronopol, ebselen, and disulfiram (Fig. 34, Table 6).

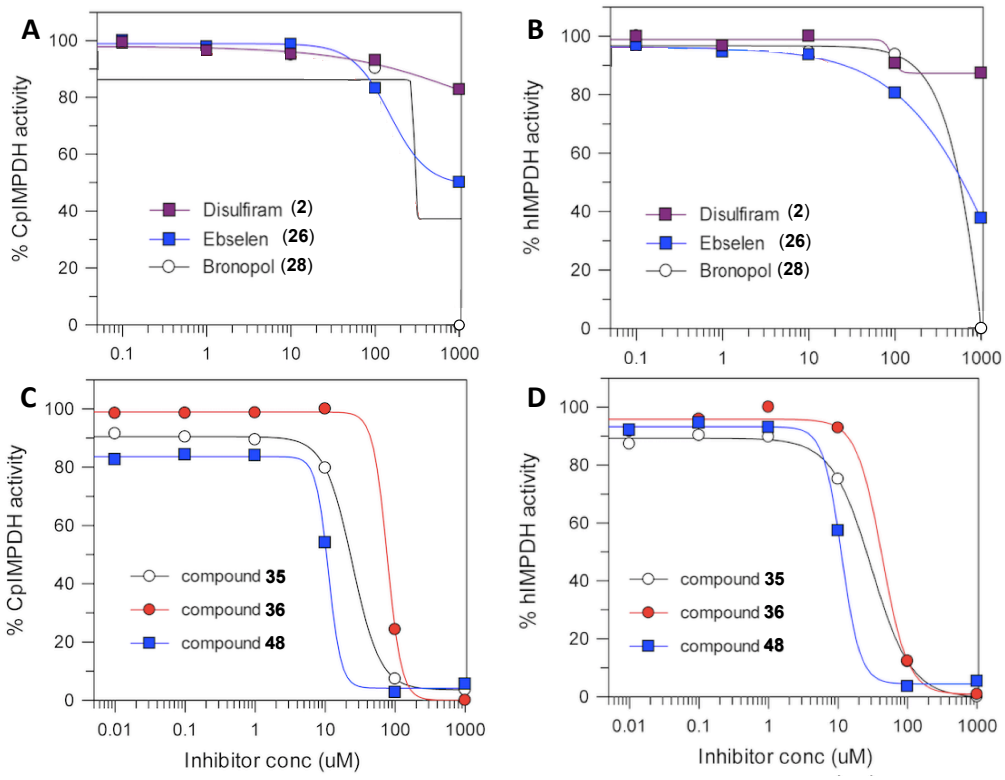


Fig. 34. Dose-dependency inhibition of hit compounds

The inhibitory of activities of hit compounds from known compound library were measured in a dose-dependent manner against CpIMPDH (A) and hIMPDH (B). Similarly, the inhibitory activities of hit compounds from synthesized compound library were measured against CpIMPDH (C) and hIMPDH (D). The NADH yield from negative control (DMSO, vehicle) was set as 100% IMPDH activity.

Furthermore, the removal of reducing agents restored the inhibitory activity of disulfiram, bronopol, and ebselen (Fig. 35, Table 6). This might be an indication that these inhibitors were reacting to the catalytic cysteine of IMPDH. In the presence of reducing agent, which also has –SH groups, the inhibitors were reacting with the reducing agents thus reducing its interaction with the enzyme. In fact, these three compounds have been reported previously as an irreversible inhibitor of cysteine, although with other different targets (Shepherd, Waigh & Gilbert, 1988; Sauna, Z. E., Peng, X., Nandigama, K., Tekle, S., Ambudkar, 2004; Picón-Camacho *et al.*, 2012; González *et al.*, 2013; Joice *et al.*, 2013; Chiou *et al.*, 2015). On the other hand, the IC_{50} value of primaquine was unaffected by the presence of DTT. Therefore, the inhibition mechanism of primaquine might be different from the other three compounds.

Interestingly, IC_{50} of the synthesized compounds did not respond in the same manner despite the similarity of their structure. The presence of methyl substitution in **36** might responsible for this behavior. However, further experiments are still necessary to confirm this.

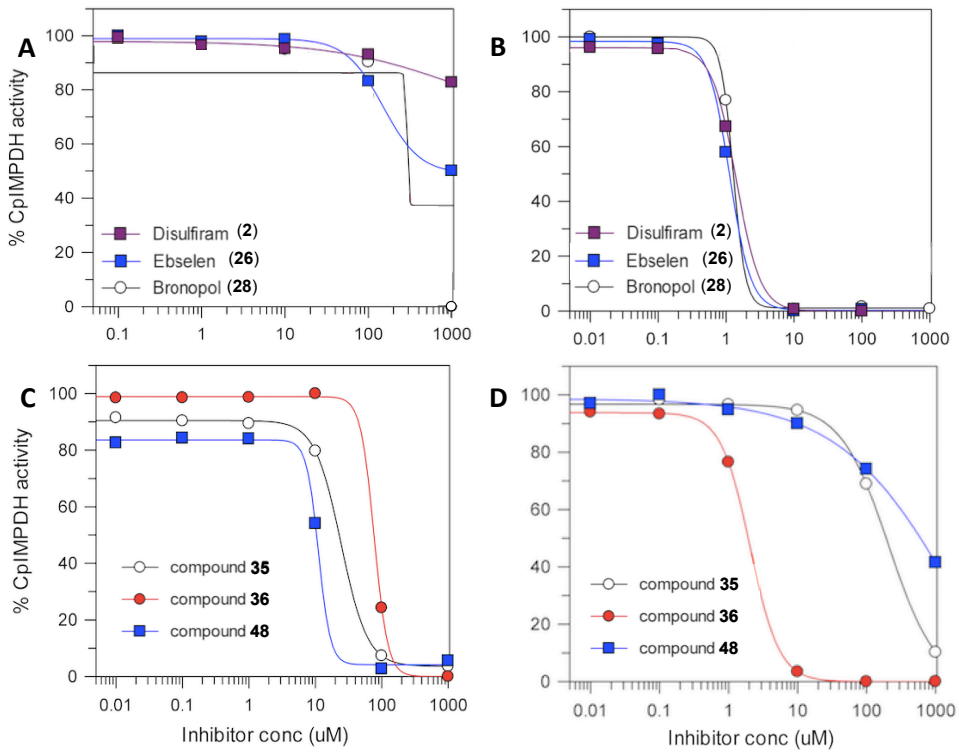


Fig. 35. Shift of IC_{50} after incubation with DTT

The inhibitory of activities of hit compounds from known compound library were measured in a dose-dependent manner against CpIMPDH, with DTT (A) and without DTT (B). Similarly, the inhibitory activities of hit compounds from synthesized compound library were measured against CpIMPDH, with DTT (C) and without DTT (D). The NADH yield from negative control (DMSO, vehicle) was set as 100% IMPDH activity.

Table 6. IC_{50} of the hit compounds (μM)

	HTS without DTT (Chemiluminescence)	LTS – Fluorescence		
		CpIMPDH (0.15 μg/ml)		hIMPDH (0.75 μg/ml)
		with DTT	without DTT	with DTT
Disulfiram (**2**)	1.5	>500.0	1.4	>500.0
Ebselen (**26**)	5.8	148.7	1.1	>500.0
Bronopol (**28**)	2.0	291.0	1.3	>500.0
35	1.1	24.4	209.8	30.3
36	1.3	76.8	2.1	43.0
48	1.0	11.1	>500.0	11.3

3.3.2. Determination of inhibition irreversibility

The enzyme was incubated with the inhibitors, with concentration of the inhibitor up to 800-times the concentration of the enzyme. Excessive inhibitor concentration ensured the maximum interaction between enzyme and inhibitor. The solution mixture was then dialyzed, so that the inhibitors were diluted up to 10^4-times. The dialysis was expected to reduce the concentration of the inhibitor to less than 10% of the enzyme concentration. Therefore, in the case of reversible inhibition, the enzyme should regain its activity. In contrast, irreversible inhibition of the enzyme will not restore the enzyme activity.

After the dialysis, the enzyme concentration in each sample was reconfirmed with Bradford staining, to ensure no leakage happened during dialysis. The enzyme activity of each sample was then measured by monitoring its time-course NADH production. The recovery of IMPDH activity in inhibitor-incubated enzyme was compared against DMSO-incubated enzyme.

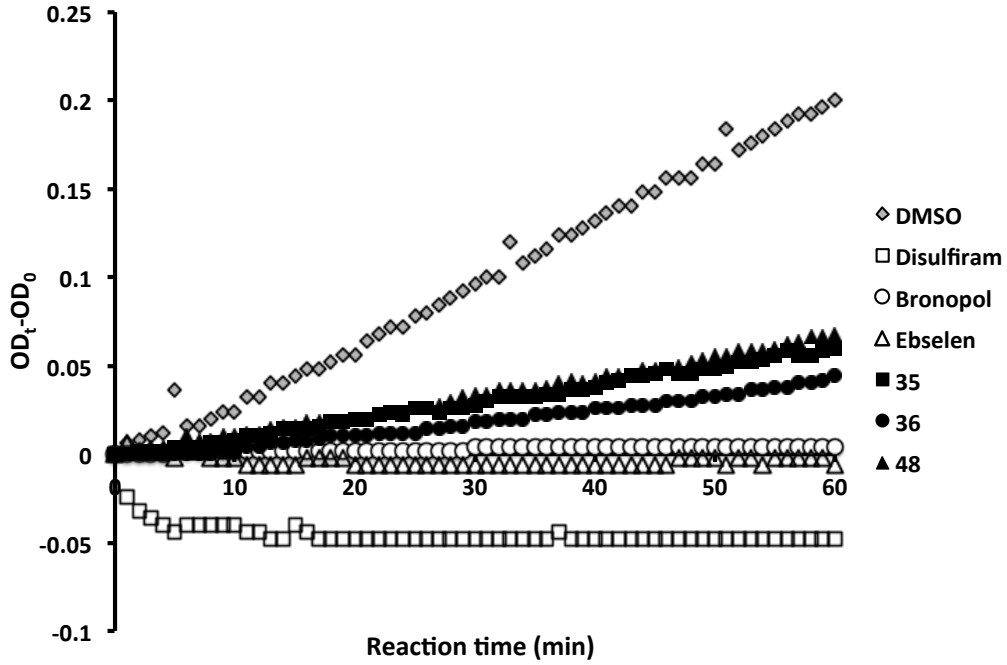


Fig. 36. Dialysis experiment for detection of inhibition irreversibility

Post-dialysis CpIMPDH was subjected into IMPDH reaction assay. CpIMPDH incubated with disulfiram, bronopol, and ebselen did not produce any increase in OD_{340}. CpIMPDH incubated with compounds **35**, **36**, and **48** showed a partial recovery of IMPDH activity. DMSO was used as negative control. OD_t is OD_{340} at time t, OD_0 is OD_{340} at time 0.

The time-course showed that the enzyme incubated with compounds **2**, **26**, and **28** failed to recover its activity after dialysis (Fig. 36). Therefore, the inhibition of IMPDH by these compounds might be irreversible. However, dialysis partially restored IMPDH activity upon inhibition by compounds **35**, **36**, and **48**. Hence, these compounds might be tight binding reversible inhibitors.

In this study, characterization of inhibitory activity by compounds **2**, **26**, and **28** was conducted as described in section 2.6 of this chapter.

3.4. The analysis of IMPDH inhibition by disulfiram and bronopol

3.4.1. Substrate protection analysis of disulfiram and bronopol

The experiment was aimed to determine the binding site inactivated by the inhibitor. In principle, the higher the concentration of the substrate which compete with the inhibitor, the lower the inactivation rate of the inhibitor. For both disulfiram (**2**) and bronopol (**28**), a higher IMP concentration protects CpIMPDH from inhibition rather than a higher concentration of NAD^+ (Fig. 37, Table 7). This implied that the inactivation by disulfiram and bronopol was accomplished by the inhibition of the IMP binding site in IMPDH. This result is in agreement with the previous hypothesis that these compounds inhibit IMPDH by reacting to cysteine residue in the IMP binding site.

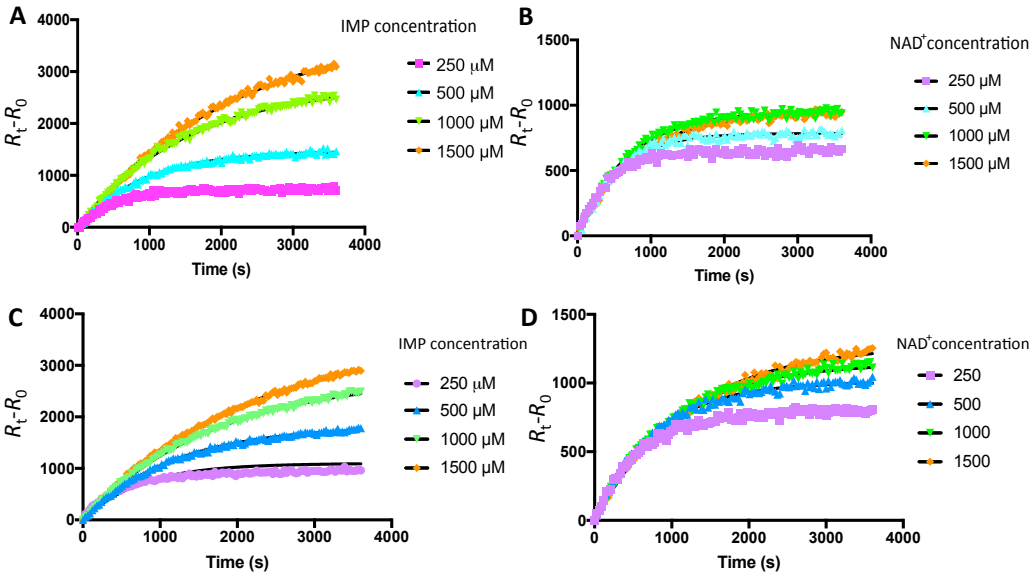


Fig. 37. Substrate protection against disulfiram and bronopol

The exponential decay of CpIMPDH activity from the inactivation by disulfiram and bronopol was monitored in an increasing concentration of the substrates. In brief, 2 µM of disulfiram was incubated with an appropriate amount of enzyme, in various IMP (A) and NAD^+ (B) concentration. In the same manner, 2 µM of bronopol was tested in various IMP (C) and NAD^+ (D) concentration. R_t is the fluorescence at time t, R_0 is the initial fluorescence at time 0. R_t-R_0 values then fitted to Eq. 3.

Table 7. Substrate protection against disulfiram and bronopol in CpIMPDH

IMP (μM)	NAD^+ (μM)	k_{obs} ($.10^{-4}$ s^{-1})	
		Disulfiram	Bronopol
250	500	20	20
500	500	11	9
1000	500	7	6
1500	500	5	5
250	250	25	17
250	500	19	13
250	1000	15	10
250	1500	13	8

Assay was carried out with standard IMPDH assay solution. The observed rate constants of enzyme inactivation (k_{obs}) values were acquired from fitting the data in Fig. 36 to Equation 3. The higher k_{obs} value represents the more potent inactivation.

3.4.2. The kinetics of irreversible inhibition by disulfiram and bronopol

The time-dependent inactivation of IMPDH in the presence of various inhibitor concentrations was also fitted into Eq. 3 (Fig. 38). The acquired k_{obs} values were then fitted into Eq. 4 (Fig. 39). Both compounds were found to be potent inhibitors of IMPDH, compared to other known irreversible IMPDH inhibitors (Table 8). However, both inhibitors showed a low selectivity between mammalian and protozoan IMPDH with k_{on} CpIMPDH:hIMPDH II value of 0.78 and 3.1 for disulfiram and bronopol, respectively. Inhibition of IMPDH by disulfiram and bronopol showed linear k_{obs} plots, which implied that the inactivation was progressed in a one-step inactivation mechanism (Fig. 40).

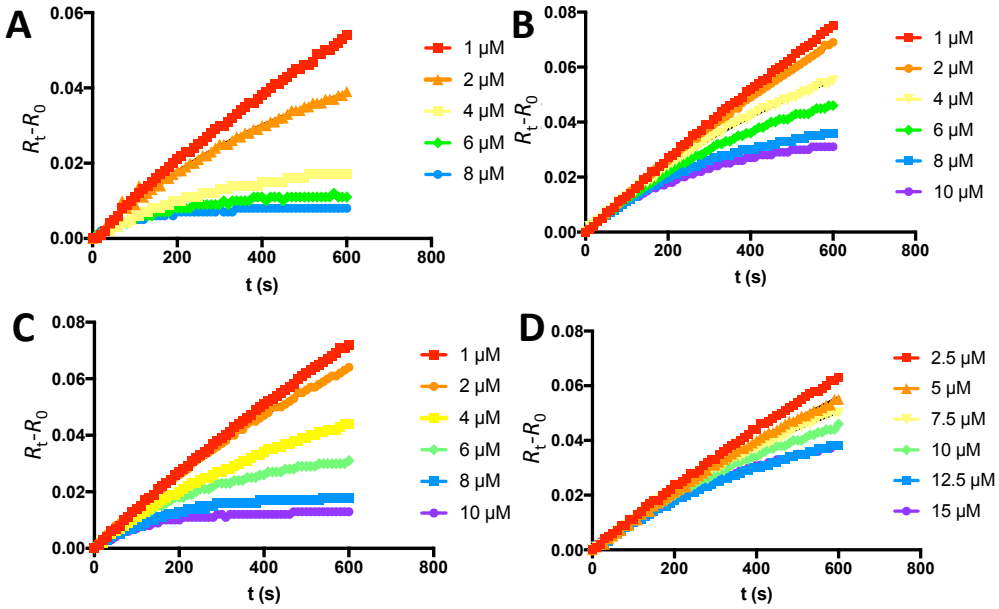


Fig. 38. Decay of enzyme activity in the presence of disulfiram and bronopol

Inhibition of CpIMPDH (A) and hIMPDH II (B) by disulfiram. The inhibition of CpIMPDH (C) and hIMPDH II (D) by bronopol. OD_{340} values were fitted to Eq. 3 to acquire k_{obs} values. Concentration values represent concentration of inhibitor compounds in the assay solution

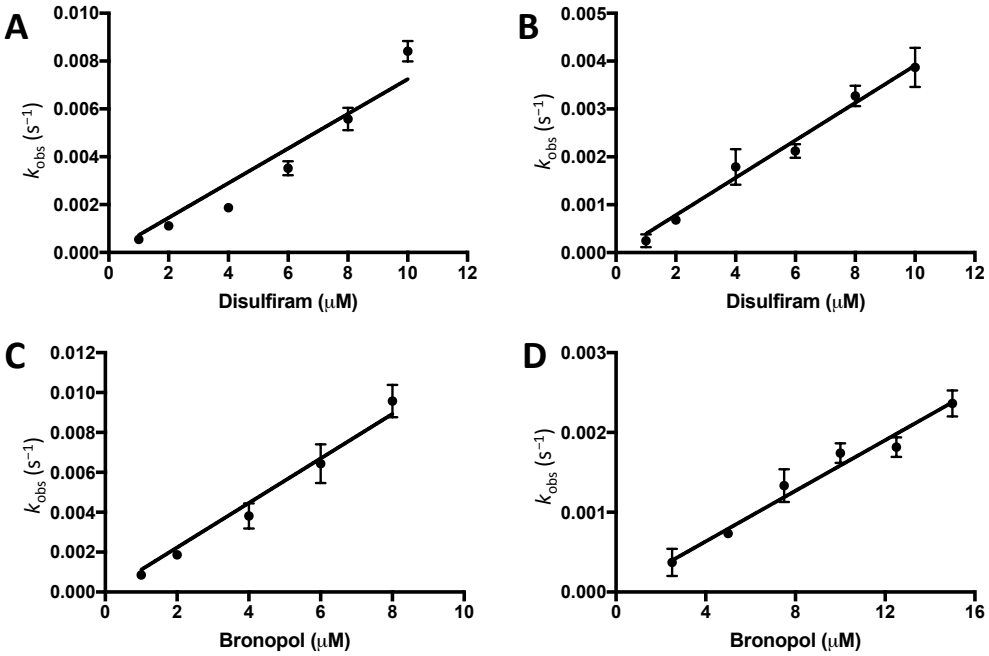


Fig. 39. The inactivation of IMPDH by disulfiram and bronopol.

Inhibition of CpIMPDH (A) and hIMPDH II (B) by disulfiram. The inhibition of CpIMPDH (C) and hIMPDH II (D) by bronopol. Values are fitted to Eq. 4. Values are mean ± SD from two independent experiments.

$$E + I \xrightarrow{k_{on}} E \bullet I^*$$

Fig. 40. One-step inactivation of enzyme

E: enzyme, I: inhibitor, E•I*: enzyme-inhibitor covalent complex

Table 8. k_{on} values of disulfiram and bronopol inhibition against IMPDHs ($M^{-1}.s^{-1}$)

	CpIMPDH	hIMPDH II	*E. coli* IMPDH
Disulfiram[a]	1.4×10^4	1.8×10^4	
Bronopol[a]	2.2×10^4	0.7×10^4	
EICARMP[b]		1.7×10^3	2.3×10^4
2-VIMP[c]			7.4×10^3
2-FVIMP[d]			2.7×10^4
6-Cl-IMP[e]		44	

[a]: Activity was measured at 30°C, 50 mM Tris-HCl buffer pH 8.0, 100 mM KCl, 3 mM EDTA, and 0.1 mg/ml BSA. CpIMPDH: 500 µM NAD^+, 250 µM IMP. hIMPDH II: 100 µM NAD^+, 250 µM IMP.

[b]: Activity was measured at 25°C, 50 mM Tris-HCl buffer pH 8.0, 100 mM KCl, 3 mM EDTA, 1 mM DTT. hIMPDH II: 100 µM NAD^+, 125 µM IMP, *E. coli* IMPDH: 2500 µM NAD^+, 1000 µM IMP (Wang *et al.*, 1996).

[c]: Activity was measured at 25°C, 50 mM Tris-HCl buffer pH 8.0, 150 mM KCl, 1 mM EDTA, 1 mM DTT. *E. coli* IMPDH: 1500 µM NAD^+, 500 µM IMP (Pal, Bera & Nair, 2002).

[d]: Activity was measured at 25°C, 100 mM Tris-HCl buffer pH 8.0, 150 mM KCl, 1 mM EDTA, 1 mM DTT. *E. coli* IMPDH: 2500 µM NAD^+, 1000 µM IMP (Nair & Kamboj, 2003).

[e]: Activity was measured at 25°C, 100 mM Tris-HCl buffer pH 8.0, 100 mM KCl, 3 mM EDTA. hIMPDH II IMPDH: 400 µM NAD^+, 200 µM IMP (Antonino, Straub & Wu, 1994).

These results showed that disulfiram and bronopol have similar potency and inhibition mechanism. Both exhibited similar high k_{on} values, comparable to those of potent irreversible IMPDH inhibitors EICARMP and 2-FVIMP. However, selectivity of disulfiram and bronopol between mammalian and bacterial IMPDH seemed to be low. This confirms that the inhibition selectivity between mammalian and bacterial IMPDH is more likely to be achieved by targeting NAD^+ binding site instead (Hedstrom, 2009). Recently, disulfiram has been reported as anticancer agent by inhibiting NPL4, an adaptor

of p97 agregase (Skrott *et al.*, 2017). As hIMPDH II is also overexpressed in various cancer cells, it is possible that IMPDH inhibition by disulfiram might also play a role for the observed antineoplastic activities (Barnes *et al.*, 2001; Chen & Pankiewicz, 2007; Hedstrom, 2009; Fellenberg *et al.*, 2010; Xu *et al.*, 2017).

This study is the first report on disulfiram and bronopol as potent IMPDH inhibitors. Previously, disulfiram has been known as an alcohol aversion drug which acts as inactivator of acetaldehyde dehydrogenase. Taking disulfiram with alcohol resulted in accumulation of acetaldehyde, causing discomforting symptoms thus discouraging further intake (Koppaka *et al.*, 2012). Bronopol on the other hand was utilized as antiseptic and antifungal compound in aquatic veterinary settings and preservative in cosmetic products (Picón-Camacho *et al.*, 2012; González *et al.*, 2013).

3.5. The analysis of IMPDH inhibition by ebselen

3.5.1. The kinetics of reversible CpIMPDH inhibition by ebselen

Ebselen showed a quite different inhibition property compared with the other two inhibitors. Ebselen did not show any irreversibility against CpIMPDH, even after decreasing the amount of enzyme and extending the measurement time (Fig. 41). The inhibition to CpIMPDH was then regarded as a reversible inhibition. This finding is particularly interesting, because previously ebselen has shown irreversible inhibition in the dialysis experiment (Fig. 36).

There are at least three possible explanations for this: First, that there are substantial differences of binding sites between IMPDHs in regards to ebselen binding; the second, that ebselen has a critical concentration threshold that triggers the chemical reactivity with cysteine residues if trespassed; and the third, that ebselen is a very slow but tight binding inhibitor of CpIMPDH (Morrison & Walsh, 2006). To confidently confirm the actual

basis of this unique modal alteration, further experiments such as crystallization study in different ratio of enzyme-inhibitor concentration are necessary. The ambivalence in the inhibition mode of ebselen has also been reported by other research groups (Walther *et al.*, 1999; Mukherjee *et al.*, 2014; Węglarz-Tomczak *et al.*, 2016).

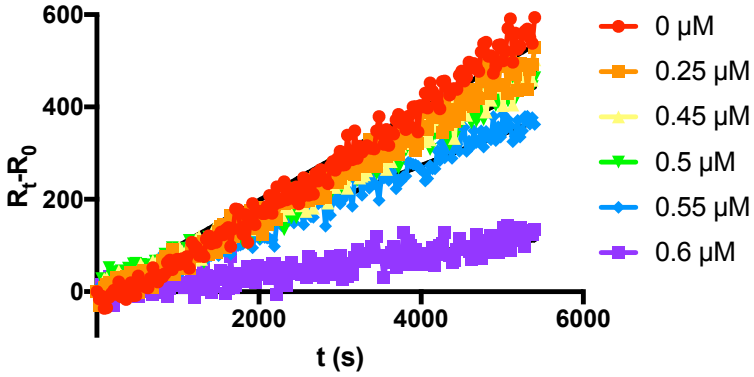


Fig. 41. Ebselen reversibly inhibit CpIMPDH.

No exponential enzyme decay was observed even after reducing enzyme concentration for 500 times and elongating the reaction time for 9 times. Concentration values represent ebselen concentration in assay solution. Assay was carried out with standard IMPDH assay solution described in Material and Method.

Michaelis-Menten plot in the absence and presence of inhibitor was fitted with Eq. 5 and 6. Ebselen inhibition to CpIMPDH was found to be noncompetitive in respect to NAD^+ and mixed in respect to IMP (Fig. 42). The noncompetitive inhibition against NAD^+ is a common characteristic of an IMP binding site inhibitor. However, mixed-model inhibition in respect to IMP implied the complex mechanism of ebselen binding to the IMP binding site. The fitted K_{is} value was much lower than the K_{ii} value, indicating a stronger affinity of ebselen to free enzymes rather than to enzyme-IMP complexes (Table 9). Taken together, the result indicated that ebselen is a reversible IMP binding site inhibitor of CpIMPDH.

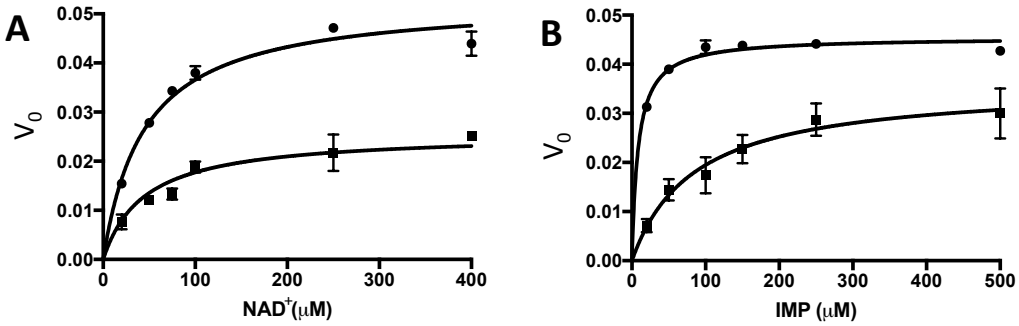


Fig. 42. Kinetics of ebselen inhibition of CpIMPDH.

The inhibition plot in respect to NAD^+, IMP concentration was kept constant at 250 μM (A). The inhibition plot in respect to IMP, NAD^+ concentration was kept constant at 400 μM (B). Circles show the assay with only vehicle and squares show the assay in the presence of 0.75 μM ebselen. Velocity (V_0) is in arbitrary units. Values are mean ± SD from two independent experiments.

Table 9. Kinetics of ebselen inhibition against CpIMPDH

C: competitive, UC: uncompetitive, NC: noncompetitive, MM: mixed model inhibition

	CpIMPDH
	706 (NC, NAD^+)
Ebselen (nM)[a]	64.6 ± 16 (K_{is}, MM, IMP)
	2808 ± 927 (K_{ii}, MM, IMP)
MPA (nM)[b]	9300 (UC, NAD^+)
GMP (μM)[b]	46 (C, IMP)

[a]: Activity was measured at 30°C, 50 mM Tris-HCl buffer pH 8.0, 100 mM KCl, 3 mM EDTA, and 0.1 mg/ml BSA. Assay against NAD^+, constant IMP at 250 μM, varied NAD^+. Assay against IMP, constant NAD^+ at 500 μM, varied IMP.

[b]: Activity was measured at 25°C, 50 mM Tris-HCl buffer pH 8.0, 100 mM KCl, 3 mM EDTA, and 1 mM DTT. Assay against NAD^+, constant IMP at 250 μM, varied NAD^+. Assay against IMP, constant NAD^+ at 500 μM, varied IMP (Umejiego *et al.*, 2004).

In contrast to CpIMPDH, inhibition of ebselen to hIMPDH was clearly showing enzymatic decay. Therefore, the inhibition was characterized in the same manner as disulfiram and bronopol.

3.5.2. Substrate protection analysis of ebselen

Similar to the previous two inhibitors, substrate protection test against ebselen inactivation was performed. The inhibition of ebselen was also found to be attenuated in the presence of high concentration IMP (Fig. 43, table 10).

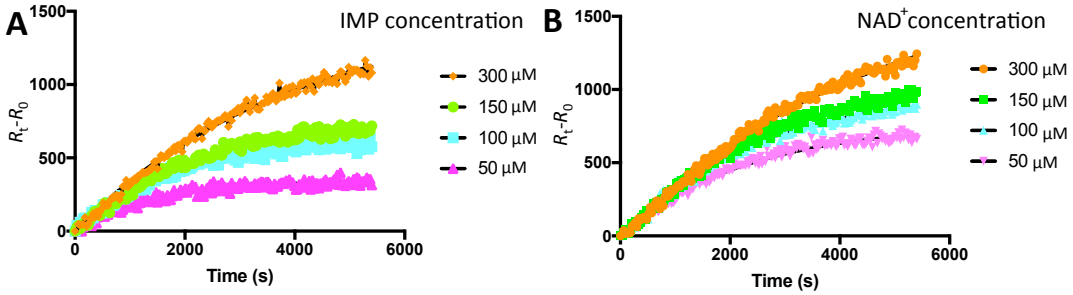


Fig. 43. Substrate protection against ebselen

The exponential decay of hIMPDH activity from the inactivation by ebselen was monitored in an increasing concentration of substrates. In brief, 2 μM of disulfiram was incubated with an appropriate amount of enzyme, in various IMP (A) and NAD^+ (B) concentration. R_t is the fluorescence at time t, R_0 is the initial fluorescence at time 0.

Table 10. Substrate protection against ebselen inactivation in hIMPDH II

IMP (μM)	NAD^+ (μM)	k_{obs} ($.10^{-4}$ s^{-1})
50	300	8
100	300	6
150	300	4
300	300	2
300	50	5
300	100	4
300	150	3
300	300	2

Assay was carried out with standard IMPDH assay solution. The observed rate constant of enzyme inactivation (k_{obs}) values was acquired from fitting the data in Fig. 42 to Equation 3. The higher k_{obs} value represents the more potent inactivation.

3.5.3. The kinetics of irreversible hIMPDH II inhibition by ebselen

Irreversible inhibition of ebselen to hIMPDH II was very interesting, due to the hyperbolic k_{obs} versus inhibitor concentration plot. Forcing this plot into Eq. 2 yielded k_{on} value of 9.3 x 10^4 $M^{-1}.s^{-1}$ (Fig. 44 and Table 11).

Therefore, the mode of IMPDH inhibition by ebselen seemed to be that of mixed mechanisms, alternating between reversible and irreversible, depending on the assay condition. Lower concentration of inhibitor might have reversible inhibition as the main mode, hence the low k_{obs} value, and the irreversible inhibition mode was progressively become more dominant as the inhibitor concentration increase. Ebselen inactivates hIMPDH II at sub-micromolar level, and might be the most potent irreversible inhibitor of IMPDH reported to date.

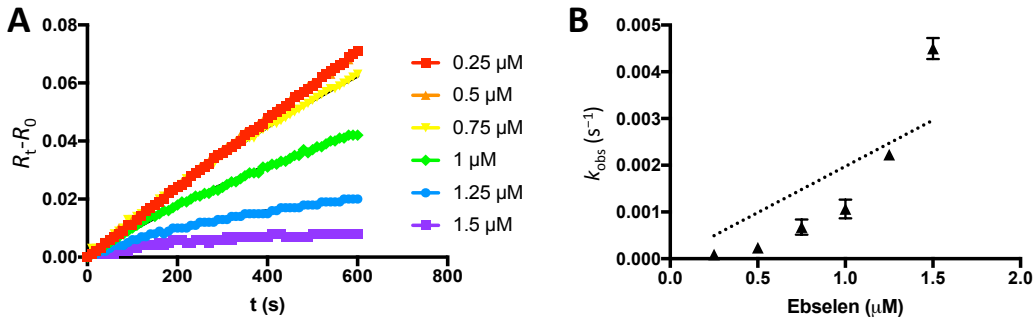


Fig. 44. The inactivation of hIMPDH II by ebselen

(A) Decay of hIMPDH II activity in the presence of ebselent. Concentration values represent concentration of ebselen in the assay solution. OD_{340} values were then fitted into Eq. 3. (B) Plot of second-order rate of inactivation (k_{on}) was acquired by fitted k_{obs} values and inhibitor concentration to Eq. 4.

Table 11. k_{on} values of ebselen against hIMPDHs ($M^{-1}.s^{-1}$)

	hIMPDH II
Ebselen[a]	> 9.3 x 10^4

[a]: Activity was measured at 30°C, 50 mM Tris-HCl buffer pH 8.0, 100 mM KCl, 3 mM EDTA, and 0.1 mg/ml BSA. CpIMPDH: 500 μM NAD^+, 250 μM IMP. hIMPDH II: 100 μM NAD^+, 250 μM IMP.

Previously, ebselen has been known as an organoselenium compound with broad reported activities, such as anti-inflammatory, anti-atherosclerotic, antibacterial, and anticancer agent (Schewe, 1995; Sharma *et al.*, 2008; Tewari *et al.*, 2009; Azad & Tomar, 2014; Thangamani, Younis & Seleem, 2015). This compound has been subjected into clinical trials as a treatment for acute ischemic stroke and a prophylactic neuroprotective agent (Saito *et al.*, 1998; Yamaguchi *et al.*, 1998). Generally regarded as a low toxicity selenium-containing compound, ebselen is exerting adverse effects only in the high concentrations (Schewe, 1995; Parnham & Sies, 2013; Azad & Tomar, 2014). Ebselen

reacts with cysteine residue of various protein, forming a selenyl-sulfide conjugation (Walther *et al.*, 1999; Ouertatani-Sakouhi *et al.*, 2010; Joice *et al.*, 2013; Lu *et al.*, 2013; Chiou *et al.*, 2015). Selenium inhibition to mice model *C. parvum* infection has been reported before but without any target validation study (Huang & Yang, 2002). Therefore, IMPDH might possibly be the molecular target of this inhibition.

3.6. Docking of hit compounds to hIMPDH II

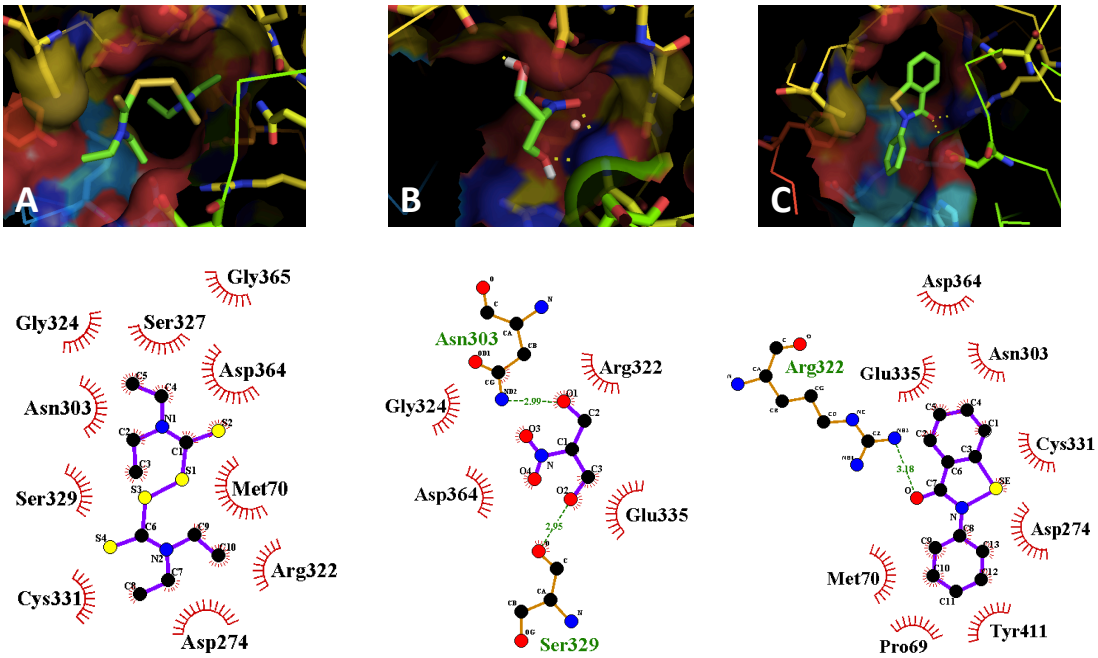


Fig. 45. Molecular docking of hit compounds to hIMPDH II

Disulfiram (A), bronopol (B), and ebselen (C) were docked into x-ray crystal of hIMPDH II. 3D interaction with IMP binding site was depicted with PyMol (top), the schematic hydrophobic interaction and hydrogen bonds were illustrated with LigPlus (bottom). hIMPDH residues that interact with inhibitor by hydrophobicity are written in black, residues that interact by hydrogen bond are written in green.

The three inhibitors were docked into hIMPDH II, with docking site including both IMP binding site and NAD^+ binding site. Docking to CpIMPDH crystal was not

performed due to the absence of catalytic Cys331 (hIMPDH II numbering) in the available CpIMPDH crystals. The previous biochemical experiment showed that this residue might play important role on the inhibitory activity of the inhibitors. However, all IMPDH crystals lack active site loops, which also plays important role in IMPDH reactions.

The docking results showed the proposed interaction of the inhibitors to the IMP binding site of hIMPDH II. As shown in LigPlus figures, Cys331 was shown in the close proximity against S and Se atoms of disulfiram and ebselen with the distance of 4 and 3.8 Å, respectively. Br atom in bronopol showed at a further distance in 5.4 Å. Disulfiram and ebselen have been reported previously to modify cysteine residues of enzymes by forming a disulfide and selenyl-sulfide bond, respectively. This binding prediction confirmed the previous findings on the inhibition site.

3.7. Inhibition of GMPR by the hit compounds

Beside IMPDH, GMPR - another enzyme in the same purine nucleotide biosynthesis pathway, has also been explored as a drug target against various medical conditions (Bessho *et al.*, 2016; Boitz *et al.*, 2016; Liu, Luo & Luo, 2018). Furthermore, the previous study on TcGMPR in Chapter II has shown that the inhibitor of IMPDH might also inhibit GMPR. Therefore, the inhibitory activity of the hit compounds against GMPR was also investigated. The GMPR from *T. congolense* (TcGMPR) was used for the experiment.

Interestingly, the hit compounds were found to inhibit guanosine 5'-monophosphate reductase (GMPR) of *T. congolense* (Fig. 46). Similar to IMPDH, GMPR has also been reported to be dependent on catalytic cysteine for its activity (Patton *et al.*, 2011; Smith *et al.*, 2016). Therefore, it is possible that the hit compounds act as dual IMPDH-GMPR inhibitors. The decay of enzymatic activity of GMPR was not observed during the time-

dependent activity assay, implied that the inhibition against *T. congolense* GMPR was reversible. Inhibition to GMPR is important in order to completely disrupt the salvage purine nucleotide biosynthesis, since GMPR could act as a surrogate enzyme of IMPDH and GMPS in the presence of ammonia (Patton *et al.*, 2011; Sarwono *et al.*, 2017).

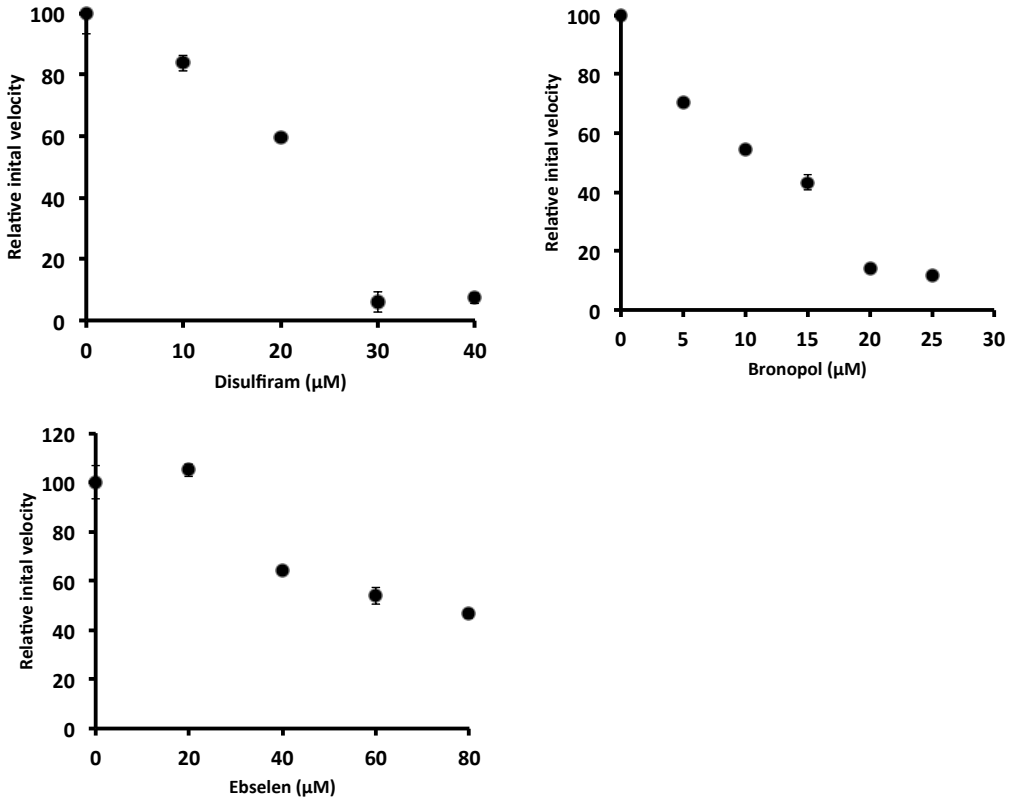


Fig. 46. Dose-dependent inhibition of hit compounds against TcGMPR

GMPR inhibitory activity was measured in assay condition described in section 2.7 of Chapter II. The initial velocity was measured as a parameter of GMPR activity. The initial velocity without inhibitor was set as 100% relative initial velocity. The values were an average of two independent experiments.

4. CONCLUSION

In conclusion, three known compounds have been repurposed from the screening of 2,660 compounds as potent novel IMPDH inhibitors: disulfiram, bronopol, and ebselen. These compounds provide novel moiety for future design of IMP binding site inhibitor, in particular to improve the selectivity of the inhibition. Aside from the utilization for chronic diseases application, the utilization of the irreversible inhibitor should be explored for anti-infective agents, especially for targeting GSH-lacking Gram-positive bacteria such as *H. pylori*, *M. tuberculosis*, *S. aureus*, and *B. subtilis* (Fahey *et al.*, 1978; Lu *et al.*, 2013).

In the follow-up study by Prof. Kentaro Kato's laboratory in National Research Center for Protozoan Diseases, Obihiro University of Agriculture and Veterinary Medicine, disulfiram and bronopol were found to exert anti-*C. parvum* activity *in vivo*. Furthermore, the characterizations of inhibitors from the synthesized compound library are currently ongoing.

5. PUBLICATIONS AND CONFERENCES

Original articles

1. **Sarwono, A.E.Y.**, Suganuma, K., Mitsuhashi, S., Okada, T., Musinguzi, S.P., Shigetomi, K., Inoue, N., Ubukata, M. 2017. Identification and characterization of guanosine 5'-monophosphate reductase of *Trypanosoma congolense* as a drug target. *Parasitol. Int.* 66:537-544. doi: 10.1016/j.parint.2017.03.006.
2. Suganuma, K., **Sarwono, A.E.Y.**, Mitsuhashi, S., Jąkalski, M., Okada, T., Nthatisi, M., Yamagishi, J., Ubukata, M, Inoue, N. 2016. Mycophenolic acid and its derivatives as potential chemotherapeutic agents targeting inosine 5'-monophosphate dehydrogenase in *Trypanosoma congolense*. *Antimicrob. Agents Chemother.* 60:4391-4393. doi: 10.1128/AAC.02816-15.

Conferences

1. **Sarwono, A.E.Y.**, Mitsuhashi, S., Bin Kabir, M.H., Shigetomi, K., Okada, T., Ohsaka, F., Otsuguro, S., Maenaka, K., Igarashi, M., Kato, K., and Ubukata, M. 2018. Identification of irreversible IMPDH inhibitors by luminescence-based high-throughput screening. Federation of European Biochemical Societies. Prague, Czech Republic.
2. **Sarwono, A.E.Y**., Suganuma, K., Mitsuhashi, S., Okada, T., Musinguzi, S.P., Shigetomi, K., Inoue, N., and Ubukata, M. 2017. GMP reductase as a drug target for chemotherapy against *T. congolense*. Japan Society for Bioscience, Biotechnology, and Agrochemistry. Kyoto, Japan.
3. **Sarwono, A.E.Y.**, Suganuma, K., Mitsuhashi, S., Shigetomi, K., Musinguzi, S.P., Shigetomi, K., Jąkalski, M., Okada, T., Nthatisi, M., Yamagishi, J., Inoue, N., Ubukata, M. 2016. Identification of novel IMP dehydrogenase and GMP reductase of *T. congolense*. Japan Society for Bioscience, Biotechnology, and Agrochemistry. Sapporo, Japan.
4. **Sarwono, A.E.Y.**, Suganuma, K., Mitsuhashi, S., Allamanda, P., Okada, T., Shigetomi, K., Shinichiro, K., Nthatisi, M., Yamagishi, J., Inoue, N., Ubukata, M. 2014. Isolation of trypanocidal compound(s) from *Todomatsu* outer bark. Japan Wood Research Society-Hokkaido Division Meeting. Sapporo, Japan.

5. **Sarwono, A.E.Y.**, Suganuma, K., Mitsuhashi, S., Allamanda, P., Okada, T., Shigetomi, K., Shinichiro, K., Nthatisi, M., Yamagishi, J., Inoue, N., Ubukata, M. 2014. Study on *Todomatsu* outer bark as a potential source of trypanocidal compounds. Japan Society for Bioscience, Biotechnology, and Agrochemistry. Sapporo, Japan.

ACKNOWLEDGEMENT

First and foremost, I would like to express my gratefulness to the Ministry of Education, Culture, Sports, Science, and Technology of the Japanese Government for granting me the scholarship for pursuing Ph.D. in Hokkaido University.

I would like to thank, Prof. Makoto Ubukata, for the opportunity to study in his laboratory, for his suggestions, and for his support during my study. I sincerely acknowledged Dr. Shinya Mitsuhashi for his constructive guidance and multidisciplinary insights. I thank Dr. Kengo Shigetomi for his advices and critical reviews.

I would also appreciate Prof. Hideyuki Matsuura and Prof. Yasuyuki Hashidoko for reviewing this manuscript and advising invaluable improvements.

I also appreciate my research collaborators from Obihiro University of Agriculture and Veterinary Medicine: Prof. Noboru Inoue, Prof. Makoto Igarashi, Prof. Kentaro Kato, Dr. Tadashi Okada, Dr. Keisuke Suganuma. Furthermore, I would like to thank my research collaborators from the Faculty of Pharmaceutical Sciences, Hokkaido University: Prof. Katsumi Maenaka, Prof. Masahiro Sakaitani, Prof. Satoshi Ichikawa, Ms. Satoko Otsuguro, and Ms. Fumina Ohsaka.

Moreover, I would like to thank all my friends in Laboratory of Wood Chemistry and Chemical Biology for their assistance during my study. I am especially grateful for my friends in the House of Friendship and Marquee24 Sapporo, for providing me a home away from home.

Finally, I would like to thank my parents and family for their unceasing love and care.

REFERENCES

Andrews, S.C. & Guest, J.R. (1988). Nucleotide sequence of the gene encoding the GMP reductase of *Escherichia coli* K12. *Biochem. J.* **255**, 35–43.

Antonino, L.C., Straub, K. & Wu, J.C. (1994). Probing the active site of human IMP dehydrogenase using halogenated purine riboside 5′-monophosphates and covalent modification reagents. *Biochemistry* **33**, 1760–1765.

Azad, G.K. & Tomar, R.S. (2014). Ebselen, a promising antioxidant drug: Mechanisms of action and targets of biological pathways. *Mol. Biol. Rep.* **41**, 4865–4879.

Baici, A. (2013). Slow-onset Enzyme Inhibition and Inactivation. Proceedings of the 5th Beilstein ESCEC Symposium; Rüdesheim/Rhein, Germany: Beilstein Institute; 2012. pp. 55–73.

Barnes, B.J., Izydore, R.A., Eakin, A.E. & Hall, I.H. (2001). Induction of Tmolt4 leukemia cell death by 3,3-disubstituted-6,6-pentamethylene-1,5-diazabicyclo[3.1.0]hexane-2-4-diones: specificity for type II inosine 5'-monophasphate dehydrogenase. *J. Pharmacol. Exp. Ther.* **298**, 790–796.

Berg, J.M., Tymoczko, J.L., Stryer, L. & Stryer, L. (2002). *Biochemistry*. Editor: W.H. Freeman. Chapter 25, Nucleotide Biosynthesis.

Bessho, T., Okada, T., Kimura, C., Shinohara, T., Tomiyama, A., Imamura, A., Kuwamura, M., Nishimura, K., Fujimori, K., Shuto, S., Ishibashi, O., Kubata, B.K. & Inui, T. (2016). Novel characteristics of *Trypanosoma brucei* guanosine 5'-monophosphate reductase distinct from host animals. *PLoS Negl. Trop. Dis.* **10**, e0004339.

Boitz, J.M., Jardim, A. & Ullman, B. (2016). GMP reductase and genetic uncoupling of adenylate and guanylate metabolism in *Leishmania donovani* parasites. *Mol. Biochem. Parasitol.* **208**, 74–83.

Cao, S., Aboge, G.O., Terkawi, M.A., Zhou, M., Luo, Y., Yu, L., Li, Y., Goo, Y., Kamyingkird, K., Masatani, T., Suzuki, H., Igarashi, I., Nishikawa, Y. & Xuan, X. (2013).

Cloning, characterization and validation of inosine 5'-monophosphate dehydrogenase of *Babesia gibsoni* as molecular drug target. *Parasitol. Int.* **62**, 87–94.

CDC. (2017). Cryptosporidiosis [WWW Document]. URL https://www.cdc.gov/dpdx/cryptosporidiosis/index.html. Accessed July 4th, 2018.

Cereser, C., Boget, S., Parvaz, P. & Revol, A. (2001). Thiram-induced cytotoxicity is accompanied by a rapid and drastic oxidation of reduced glutathione with consecutive lipid peroxidation and cell death. *Toxicology* **163**, 153–162.

Chaudhary, K., Darling, J.A., Fohl, L.M., Sullivan, W.J., Donald, R.G.K., Pfefferkorn, E.R., Ullman, B. & Roost, D.S. (2004). Purine salvage pathways in the apicomplexan parasite *Toxoplasma gondii*. *J. Biol. Chem.* **279**, 31221–31227.

Chen, L. & Pankiewicz, K.W. (2007). Recent development of IMP dehydrogenase inhibitors for the treatment of cancer. *Curr. Opin. Drug Discov. Devel.* **10**, 403–412.

Chiou, J., Wan, S., Chan, K.F., So, P.K., He, D., Chan, E.W., Chan, T., Wong, K., Tao, J. & Chen, S. (2015). Ebselen as a potent covalent inhibitor of New Delhi metallo-β-lactamase (NDM-1). *Chem. Commun.* **51**, 9543–9546.

Chitanga, S., Marcotty, T., Namangala, B., van den Bossche, P., van den Abbeele, J. & Delespaux, V. (2011). High prevalence of drug resistance in animal trypanosomes without a history of drug exposure. *PLoS Negl. Trop. Dis.* **5**, e1454.

Codjia, V., Mulatu, W., Majiwa, P.A.O., Leak, S.G.A., Rowlands, G.J., Authié, E., d'Ieteren, G.D.M. & Peregrine, A.S. (1993). Epidemiology of bovine trypanosomiasis in the Ghibe valley, southwest Ethiopia. 3. Occurrence of populations of *Trypanosoma congolense* resistant to diminazene, isometamidium and homidium. *Acta Trop.* **53**, 151–163.

Cox, J.A.G., Mugumbate, G., Del Peral, L.V.G., Jankute, M., Abrahams, K.A., Jervis, P., Jackenkroll, S., Perez, A., Alemparte, C., Esquivias, J., Lelièvre, J., Ramon, F., Barros, D., Ballell, L. & Besra, G.S. (2016). Novel inhibitors of *Mycobacterium tuberculosis* GuaB2 identified by a target based high-throughput phenotypic screen. *Sci. Rep.* **6**, 38986,

1–10.

Cuny, G.D., Suebsuwong, C. & Ray, S.S. (2017). Inosine-5'-monophosphate dehydrogenase (IMPDH) inhibitors: a patent and scientific literature review (2002–2016). *Expert Opin. Ther. Pat.* **27**, 677–690.

Delespaux, V., Vitouley, H.S., Marcotty, T., Speybroeck, N., Berkvens, D., Roy, K., Geerts, S. & van den Bossche, P. (2010). Chemosensitization of *Trypanosoma congolense* strains resistant to isometamidium chloride by tetracyclines and enrofloxacin. *PLoS Negl. Trop. Dis.* **4**, e828.

Deng, Y., Wang, Z., Ying, K., Gu, S., Ji, C., Huang, Y., Gu, X., Wang, Y., Xu, Y., Li, Y., Xie, Y. & Mao, Y. (2002). NADPH-dependent GMP reductase isoenzyme of human (GMPR2): Expression, purification, and kinetic properties. *Int. J. Biochem. Cell Biol.* **34**, 1035–1050.

Dunkern, T., Prabhu, A., Kharkar, P.S., Goebel, H., Rolser, E., Burckhard-Boer, W., Arumugam, P. & Makhija, M.T. (2012). Virtual and experimental high-throughput screening (HTS) in search of novel inosine 5′-monophosphate dehydrogenase II (IMPDH II) inhibitors. *J. Comput. Aided. Mol. Des.* **26**, 1277–1292.

DuPont, H.L., Chappell, C.L., Sterling, C.R., Okhuysen, P.C., Rose, J.B. & Jakubowski, W. (1995). The Infectivity of *Cryptosporidium parvum* in Healthy Volunteers. *N. Engl. J. Med.* **332**, 855–859.

Fahey, R.C., Brown, W.C., Adams, W.B. & Worsham, M.B. (1978). Occurrence of glutathione in bacteria. *J. Bacteriol.* **133**, 1126–1129.

FAO. (2014). African Animal Trypanosomes [WWW Document]. URL http://www.fao.org/docrep/006/x0413e/x0413e02.htm. Accessed July 4th, 2018.

Fayer, R. (2004). *Cryptosporidium*: a water-borne zoonotic parasite. *Vet. Parasitol.* **126**, 37–56.

Fayer, R., Morgan, U. & Upton, S.J. (2000). Epidemiology of *Cryptosporidium*: transmission,

detection and identification. *Int. J. Parasitol.* **30**, 1305–22.

Fellenberg, J., Kunz, P., Sähr, H. & Depeweg, D. (2010). Overexpression of inosine 5'-monophosphate dehydrogenase type II mediates chemoresistance to human osteosarcoma cells. *PLoS One* **5**, 1–8.

Feng, B.Y., Simeonov, A., Jadhav, A., Babaoglu, K., Inglese, J., Shoichet, B.K. & Austin, C.P. (2007). A high-throughput screen for aggregation-based inhibition in a large compound library. *J. Med. Chem.* **50**, 2385–2390.

Franchetti, P. & Grifantini, M. (1999). Nucleoside and non-nucleoside IMP dehydrogenase inhibitors as antitumor and antiviral agents. *Curr. Med. Chem.* **6**, 599–614.

Gargala, G. (2008). Drug treatment and novel drug target against *Cryptosporidium*. *Parasite* **15**, 275–281.

González, Á., Celada, J.D., Melendre, P.M., Carral, J.M., Sáez-Royuela, M., González, R. & García, V. (2013). Effects of different bronopol treatments on final survival rates in the artificial incubation of crayfish eggs (*Pacifastacus leniusculus, Astacidae*). *Aquac. Res.* **44**, 354–358.

Gorla, S.K., McNair, N.N., Yang, G., Gao, S., Hu, M., Jala, V.R., Haribabu, B., Striepen, B., Cuny, G.D., Mead, J.R. & Hedstrom, L. (2014). Validation of IMP dehydrogenase inhibitors in a mouse model of cryptosporidiosis. *Antimicrob. Agents Chemother.* **58**, 1603–1614.

Hammond, D.J. & Gutteridge, W.E. (1984). Purine and pyrimidine metabolism in the *Trypanosomatidae*. *Mol. Biochem. Parasitol.* **13**, 243–261.

Hawking, F. (1978). The resistance of *Trypanosoma congolense*, *T. vivax* and *T. evansi* to human plasma. *Trans. R. Soc. Trop. Med. Hyg.* **72**, 405–407.

Hedstrom, L. (2009). IMP dehydrogenase: mechanism of action and inhibition. *Chem. Rev.* **109**, 2903–2928.

Hedstrom, L. (2012). The dynamic determinants of reaction specificity in the IMPDH/GMPR

family of $(\beta/\alpha)_8$ barrel enzymes. *Crit. Rev. Biochem. Mol. Biol.* **47**, 250–263.

Hedstrom, L., Liechti, G., B. Goldberg, J. & R. Gollapalli, D. (2011). The antibiotic potential of prokaryotic IMP dehydrogenase inhibitors. *Curr. Med. Chem.* **18**, 1909–1918.

Huang, K. & Yang, S. (2002). Inhibitory effect of selenium on *Cryptosporidium parvum* infection *in vitro* and *in vivo*. *Biol. Trace Elem. Res.* **90**, 261–272.

Hunter, P.R. & Nichols, G. (2002). Epidemiology and clinical features of *Cryptosporidium* infection in immunocompromised patients. *Clin. Microbiol. Rev.* **15**, 145–154.

Ignoul, S. & Eggermont, J. (2005). CBS domains: structure, function, and pathology in human proteins. *Am. J. Physiol. Cell Physiol.* **289**, C1369–C1378.

Jain, J., Almquist, S.J., Shlyakhter, D. & Harding, M.W. (2001). VX-497: A novel, selective IMPDH inhibitor and immunosuppressive agent. *J. Pharm. Sci.* **90**, 625–637.

Joice, A.C., Harris, M.T., Kahney, E.W., Dodson, H.C., Maselli, A.G., Whitehead, D.C. & Morris, J.C. (2013). Exploring the mode of action of ebselen in *Trypanosoma brucei* hexokinase inhibition. *Int. J. Parasitol. Drugs Drug Resist.* **3**, 154–160.

Joshua, R.A. (1989). Occurrence of human serum-resistant *Trypanosoma congolense* in goats and sheep in Nigeria. *Vet. Parasitol.* **31**, 107–113.

Mac Kenzie, W.R., Hoxie, N.J., Proctor, M.E., Gradus, M.S., Blair, K.A., Peterson, D.E., Kazmierczak, J.J., Addiss, D.G., Fox, K.R., Rose, J.B. & Davis, J.P. (1994). A massive outbreak in Milwaukee of *Cryptosporidium* infection transmitted through the public water supply. *N. Engl. J. Med.* **331**, 161–167.

Kondoh, T., Kanno, H., Chang, L. & Yoshida, A. (1991). Genomic structure and expression of human guanosine monophosphate reductase. *Hum. Genet.* **88**, 219–224.

Koppaka, V., Thompson, D.C., Chen, Y., Ellermann, M., Nicolaou, K.C., Juvonen, R.O., Petersen, D., Deitrich, R.A., Hurley, T.D. & Vasiliou, V. (2012). Aldehyde dehydrogenase inhibitors: a comprehensive review of the pharmacology, mechanism of action, substrate specificity, and clinical application. *Pharmacol. Rev.* **64**, 520–539.

Li, Q., Leija, C., Rijo-Ferreira, F., Chen, J., Cestari, I., Stuart, K., Tu, B.P. & Phillips, M.A. (2015). GMP synthase is essential for viability and infectivity of *Trypanosoma brucei* despite a redundant purine salvage pathway. *Mol. Microbiol.* **97**, 1006–1020.

Liechti, G. & Goldberg, J.B. (2012). *Helicobacter pylori* relies primarily on the purine salvage pathway for purine nucleotide biosynthesis. *J. Bacteriol.* **194**, 839–854.

Liu, B., Li, S. & Hu, J. (2004). Technological advances in high-throughput screening. *Am J Pharmacogenomics.* **2**, 597–603.

Liu, H., Luo, K. & Luo, D. (2018). Guanosine monophosphate reductase 1 is a potential therapeutic target for Alzheimer's disease. *Sci. Rep.* **8**: 1–10.

Lu, J., Vlamis-Gardikas, A., Kandasamy, K., Zhao, R., Gustafsson, T.N., Engstrand, L., Hoffner, S., Engman, L. & Holmgren, A. (2013). Inhibition of bacterial thioredoxin reductase: an antibiotic mechanism targeting bacteria lacking glutathione. *FASEB J.* **27**, 1394–1403.

Lucumi, E., Darling, C., Jo, H., Napper, A.D., Chandramohanadas, R., Fisher, N., Shone, A.E., Jing, H., Ward, S.A., Biagini, G.A., DeGrado, W.F., Diamond, S.L. & Greenbaum, D.C. (2010). Discovery of potent small-molecule inhibitors of multidrug-resistant *Plasmodium falciparum* using a novel miniaturized high-throughput luciferase-based assay. *Antimicrob. Agents Chemother.* **54**, 3597–3604.

Mamoudou, A., Delespaux, V., Chepnda, V., Hachimou, Z., Andrikaye, J.P., Zoli, A. & Geerts, S. (2008). Assessment of the occurrence of trypanocidal drug resistance in trypanosomes of naturally infected cattle in the Adamaoua region of Cameroon using the standard mouse test and molecular tools. *Acta Trop.* **106**, 115–118.

Martinelli, L.K.B., Ducati, R.G., Rosado, L.A., Breda, A., Selbach, B.P., Santos, D.S. & Basso, L.A. (2011). Recombinant *Escherichia coli* GMP reductase: kinetic, catalytic and chemical mechanisms, and thermodynamics of enzyme-ligand binary complex formation. *Mol. Biosyst.* **7**, 1289–1305.

Matthews, K.R. (2015). 25 years of African trypanosome research: From description to molecular dissection and new drug discovery. *Mol. Biochem. Parasitol.* **200**, 30–40.

McConkey, G.A. (2000). *Plasmodium falciparum*: isolation and characterisation of a gene encoding protozoan GMP Synthase. *Exp. Parasitol.* **94**, 23–32.

Mead, J.R. (2002). Cryptosporidiosis and the challenges of chemotherapy. *Drug Resist. Updat.* **5**, 47–57.

Minond, D., Saldanha, S.A., Subramaniam, P., Spaargaren, M., Spicer, T., Fotsing, J.R., Weide, T., Fokin, V. V., Sharpless, K.B., Galleni, M., Bebrone, C., Lassaux, P. & Hodder, P. (2009). Inhibitors of VIM-2 by screening pharmacologically active and click-chemistry compound libraries. *Bioorganic Med. Chem.* **17**, 5027–5037.

Mitsuhashi, S., Takenaka, J., Iwamori, K., Nakajima, N. & Ubukata, M. (2010). Structure-activity relationships for inhibition of inosine monophosphate dehydrogenase and differentiation induction of K562 cells among the mycophenolic acid derivatives. *Bioorganic Med. Chem.* **18**, 8106–8111.

Morrison, J.F. & Walsh, C.T. (2006). The behavior and significance of slow-binding enzyme inhibitors. In *Advances in Enzymology and Related Areas of Molecular Biology*, 201–301.

Mukherjee, S., Weiner, W.S., Schroeder, C.E., Simpson, D.S., Hanson, A.M., Sweeney, N.L., Marvin, R.K., Ndjomou, J., Kolli, R., Isailovic, D., Schoenen, F.J. & Frick, D.N. (2014). Ebselen inhibits hepatitis C virus NS3 helicase binding to nucleic acid and prevents viral replication. *ACS Chem. Biol.* **9**, 2393–2403.

Munang'Andu, H.M., Siamudaala, V.M., Munyeme, M. & Nalubamba, K.S. (2012). Detection of parasites and parasitic infections of free-ranging wildlife on a game ranch in Zambia: A challenge for disease control. *J. Parasitol. Res.* **2012**, 1–8.

Nair, V. & Kamboj, R.C. (2003). Inhibition of inosine monophosphate dehydrogenase (IMPDH) by 2-[2-(Z)-Fluorovinyl]inosine 5′-Monophosphate. *Bioorganic Med. Chem. Lett.* **13**, 645–647.

Noyes, H., Brass, A., Obara, I., Anderson, S., Archibald, A.L., Bradley, D.G., Fisher, P., Freeman, A., Gibson, J., Gicheru, M., Hall, L., Hanotte, O., Hulme, H., McKeever, D., Murray, C., Oh, S.J., Tate, C., Smith, K., Tapio, M., Wambugu, J., Williams, D.J., Agaba, M. & Kemp, S.J. (2011). Genetic and expression analysis of cattle identifies candidate genes in pathways responding to *Trypanosoma congolense* infection. *Proc. Natl. Acad. Sci.* **108**, 9304–9309.

Opperdoes, F.R. & Coombs, G.H. (2007). Metabolism of *Leishmania*: proven and predicted. *Trends Parasitol.* **23**, 149–158.

Ouertatani-Sakouhi, H., El-Turk, F., Fauvet, B., Cho, M.-K., Pinar Karpinar, D., Le Roy, D., Dewor, M., Roger, T., Bernhagen, J., Calandra, T., Zweckstetter, M. & Lashuel, H.A. (2010). Identification and characterization of novel classes of macrophage Migration Inhibitory Factor (MIF) inhibitors with distinct mechanisms of action. *J. Biol. Chem.* **285**, 26581–26598.

Pal, S., Bera, B. & Nair, V. (2002). Inhibition of inosine monophosphate dehydrogenase (IMPDH) by the antiviral compound, 2-vinylinosine monophosphate. *Bioorganic Med. Chem.* **10**, 3615–3618.

Parnham, M.J. & Sies, H. (2013). The early research and development of ebselen. *Biochem. Pharmacol.* **86**, 1248–1253.

Patton, G.C., Stenmark, P., Gollapalli, D.R., Sevastik, R., Kursula, P., Flodin, S., Schuler, H., Swales, C.T., Eklund, H., Himo, F., Nordlund, P. & Hedstrom, L. (2011). Cofactor mobility determines reaction outcome in the IMPDH and GMPR $(\beta\text{-}\alpha)_8$ barrel enzymes. *Nat. Chem. Biol.* **7**, 950–958.

Picón-Camacho, S.M., Taylor, N.G.H., Bron, J.E., Guo, F.C. & Shinn, A.P. (2012). Effects of long duration, low dose bronopol exposure on the control of *Ichthyophthirius multifiliis* (*Ciliophora*), parasitising rainbow trout (*Oncorhynchus*). *Vet. Parasitol.* **186**, 237–244.

Pua, K.H., Stiles, D.T., Sowa, M.E. & Verdine, G.L. (2017). IMPDH2 is an intracellular target

of the Cyclophilin A and Sanglifehrin A complex. *Cell Rep.* **18**, 432–442.

Ratcliffe, A.J. (2006). Inosine 5'-monophosphate dehydrogenase inhibitors for the treatment of autoimmune diseases. *Curr. Opin. Drug Discov. Devel.* **9**, 595–605.

Saito, I., Asano, T., Sano, K., Takakura, K., Abe, H., Yoshimoto, T., Kikuchi, H., Ohta, T. & Ishibashi, S. (1998). Neuroprotective effect of an antioxidant, ebselen, in patients with delayed neurological deficits after aneurysmal subarachnoid hemorrhage. *Neurosurgery* **42**, 269–278.

Sarwono, A.E.Y. (2015). Screening of antiprotozoan agents against *Trypanosoma congolense* and *Cryptosporidium parvum*. Thesis.

Sarwono, A.E.Y., Suganuma, K., Mitsuhashi, S., Okada, T., Musinguzi, S.P., Shigetomi, K., Inoue, N. & Ubukata, M. (2017). Identification and characterization of guanosine 5′-monophosphate reductase of *Trypanosoma congolense* as a drug target. *Parasitol. Int.* **66**, 537–564.

Sauna, Z. E., Peng, X., Nandigama, K., Tekle, S., Ambudkar, S. V. (2004). The molecular basis of the action of disulfiram as a modulator of the multidrug resistance-linked ATP Binding Cassette Transporters MDR1 (ABCB1) and MRP1 (ABCC1). *Mol. Pharmacol.* **65**, 675–684.

Schewe, T. (1995). Molecular actions of Ebselen - An antiinflammatory antioxidant. *Gen. Pharmacol.* **26**, 1153–1169.

Sharma, V., Tewari, R., Sk, U.H., Joseph, C. & Sen, E. (2008). Ebselen sensitizes glioblastoma cells to Tumor Necrosis Factor (TNF alpha)-induced apoptosis through two distinct pathways involving NF-kappa B downregulation and Fas-mediated formation of death inducing signaling complex. *Int. J. Cancer* **123**, 2204–2212.

Shepherd, J.A., Waigh, R.D. & Gilbert, P. (1988). Antibacterial action of 2-bromo-2-nitropropane-1,3-diol (bronopol). *Antimicrob. Agents Chemother.* **32**, 1693–1698.

Siles, S.A., Srinivasan, A., Pierce, C.G., Lopez-Ribot, J.L. & Ramasubramanian, A.K. (2013).

High-throughput screening of a collection of known pharmacologically active small compounds for identification of *Candida albicans* biofilm inhibitors. *Antimicrob. Agents Chemother.* **57**, 3681–3687.

Skrott, Z., Mistrik, M., Andersen, K.K., Friis, S., Majera, D., Gursky, J., Ozdian, T., Bartkova, J., Turi, Z., Moudry, P., Kraus, M., Michalova, M., Vaclavkova, J., Dzubak, P., Vrobel, I., Pouckova, P., Sedlacek, J., Miklovicova, A., Kutt, A., Li, J., Mattova, J., Driessen, C., Dou, Q.P., Olsen, J., Hajduch, M., Cvek, B., Deshaies, R.J. & Bartek, J. (2017). Alcohol-abuse drug disulfiram targets cancer via p97 segregase adaptor NPL4. *Nature* **552**, 194–199.

Smith, S., Boitz, J., Chidambaram, E.S., Chatterjee, A., Ait-Tihyaty, M., Ullman, B. & Jardim, A. (2016). The cystathionine- β -synthase domains on the guanosine 5′-monophosphate reductase and inosine 5′-monophosphate dehydrogenase enzymes from *Leishmania* regulate enzymatic activity in response to guanylate and adenylate nucleotide levels. *Mol. Microbiol.* **100**, 824–840.

Spector, T. & Jones, T.E. (1982). Guanosine 5'-monophosphate reductase from *Leishmania donovani*. A possible chemotherapeutic target. *Biochem. Pharmacol.* **31**, 3891–3897.

Suganuma, K., Sarwono, A.E.Y., Mitsuhashi, S., Jakalski, M., Okada, T., Nthatisi, M., Yamagishi, J., Ubukata, M. & Inoue, N. (2016). Mycophenolic acid and its derivatives as potential chemotherapeutic agents targeting inosine monophosphate dehydrogenase in *Trypanosoma congolense*. *Antimicrob. Agents Chemother.* **60**, 4391–4393.

Tewari, R., Sharma, V., Koul, N., Ghosh, A., Joseph, C., Hossain Sk, U. & Sen, E. (2009). Ebselen abrogates TNFα induced pro-inflammatory response in glioblastoma. *Mol. Oncol.* **3**, 77–83.

Thangamani, S., Younis, W. & Seleem, M.N. (2015). Repurposing clinical molecule ebselen to combat drug resistant pathogens. *PLoS One* **10**, e0133877, 1–16.

Tong, X., Smith, J., Bukreyeva, N., Koma, T., Manning, J.T., Kalkeri, R., Kwong, A.D. &

Paessler, S. (2018). Merimepodib, an IMPDH inhibitor, suppresses replication of Zika virus and other emerging viral pathogens. *Antiviral Res.* **149**, 34–40.

Truc, P., Büscher, P., Cuny, G., Gonzatti, M.I., Jannin, J., Joshi, P., Juyal, P., Lun, Z.R., Mattioli, R., Pays, E., Simarro, P.P., Teixeira, M.M.G., Touratier, L., Vincendeau, P. & Desquesnes, M. (2013). Atypical human infections by animal trypanosomes. *PLoS Negl. Trop. Dis.* **7**, e2256, 1–7.

Ullman, B., Carter, N.S., Yates, P., Arendt, C.S. & Boitz, J.M. (2008). Purine and pyrimidine metabolism in *Leishmania*. *Adv. Exp. Med. Biol.* **625**, 141–154.

Umejiego, N.N., Gollapalli, D., Sharling, L., Volftsun, A., Lu, J., Benjamin, N.N., Stroupe, A.H., Riera, T. V., Striepen, B. & Hedstrom, L. (2008). Targeting a prokaryotic protein in a eukaryotic pathogen: identification of lead compounds against cryptosporidiosis. *Chem. Biol.* **15**, 70–77.

Umejiego, N.N., Li, C., Riera, T., Hedstrom, L. & Striepen, B. (2004). *Cryptosporidium parvum* IMP dehydrogenase - Identification of functional, structural, and dynamic properties that can be exploited for drug design. *J. Biol. Chem.* **279**, 40320–40327.

Vertommen, D., Van Roy, J., Szikora, J.P., Rider, M.H., Michels, P.A.M. & Opperdoes, F.R. (2008). Differential expression of glycosomal and mitochondrial proteins in the two major life-cycle stages of *Trypanosoma brucei*. *Mol. Biochem. Parasitol.* **158**, 189–201.

Walther, M., Holzhütter, H.G., Kuban, R.J., Wiesner, R., Rathmann, J. & Kühn, H. (1999). The inhibition of mammalian 15-lipoxygenases by the anti-inflammatory drug ebselen: dual-type mechanism involving covalent linkage and alteration of the iron ligand sphere. *Mol. Pharmacol.* **56**, 196–203.

Wang, W. & Hedstrom, L. (1997). Kinetic mechanism of human inosine 5'-monophosphate dehydrogenase type II: Random addition of substrates and ordered release of products. *Biochemistry* **36**, 8479–8483.

Wang, W., Papov, V. V, Minakawa, N., Matsuda, Biemann, K. & Hedstrom, L. (1996).

Inactivation of inosine 5'-monophosphate dehydrogenase by the antiviral agent 5-ethynyl-1-beta-D-ribofuranosylimidazole-4-carboxamide 5'-monophosphate. *Biochemistry* **35**, 95–101.

Węglarz-Tomczak, E., Burda-Grabowska, M., Giurg, M. & Mucha, A. (2016). Identification of methionine aminopeptidase 2 as a molecular target of the organoselenium drug ebselen and its derivatives/analogues: Synthesis, inhibitory activity and molecular modeling study. *Bioorganic Med. Chem. Lett.* **26**, 5254–5259.

Xiang, B., Taylor, J.C. & Markham, G.D. (1996). Monovalent cation activation and kinetic mechanism of inosine 5'-monophosphate dehydrogenase. *J. Biol. Chem.* **271**, 1435–1440.

Xu, Y., Zheng, Z., Gao, Y., Duan, S., Chen, C., Rong, J., Wang, K., Yun, M., Weng, H., Ye, S. & Zhang, J. (2017). High expression of IMPDH2 is associated with aggressive features and poor prognosis of primary nasopharyngeal carcinoma. *Sci. Rep.* **7**, 1–10.

Yamaguchi, T., Sano, K., Takakura, K., Saito, I., Shinohara, Y., Asano, T. & Yasuhara, H. (1998). Ebselen in acute ischemic stroke : A placebo-controlled, double-blind clinical trial. *Stroke* **29**, 12–17.

Yoshida, N. & Plessmann Camargo, E. (1978). Ureotelism and ammonotelism in trypanosomatids. *J. Bacteriol.* **136**, 1184–1186.

Zahnle, K.J. (2006). Earth's earliest atmosphere. *Elements* **2**, 217–222.

Zeuthen, T., Wu, B., Pavlovic-Djuranovic, S., Holm, L.M., Uzcategui, N.L., Duszenko, M., Kun, J.F.J., Schultz, J.E. & Beitz, E. (2006). Ammonia permeability of the aquaglyceroporins from *Plasmodium falciparum*, *Toxoplasma gondii* and *Trypansoma brucei*. *Mol. Microbiol.* **61**, 1598–1608.

Zhang, J.-H., Chung, T.D.Y. & Oldenburg, K.R. (1999). A simple statistical parameter for use in evaluation and validation of high throughput screening assays. *J. Biomol. Screen.* **4**, 67–73.

Zhou, X., Cahoon, M., Rosa, P. & Hedstrom, L. (1997). Expression, purification, and

characterization of inosine 5’-monophosphate dehydrogenase from *Borrelia burgdorferi*. *J. Biol. Chem.* **272**, 21977–21981.

APPENDIXES

Fig. S1. **Validation of HTS against IMPDH**

To establish z'-factor of the HTS model, 100 nl of 200 mM MPA (positive control) or DMSO (vehicle) was added to 384-wells plate with Mosquito LCP. Subsequently, 10 µl of reaction solution and 10 µl of start solution were added to each well with Multidrop Combi. Incubation was carried out at 30°C, 30 min, in the dark.

Z'-factor value is defined as: Z'-factor $=1-[(3\sigma c^{-} + 3\sigma c^{+})/(\mu c^{-} - \mu c^{+})]$; where σc^{-} and μc^{-} denote standard deviation and mean signal value of assay samples with only vehicle, respectively, and σc^{+} and μc^{+} each denote standard deviation and mean signal value of assay samples with reference inhibitors.

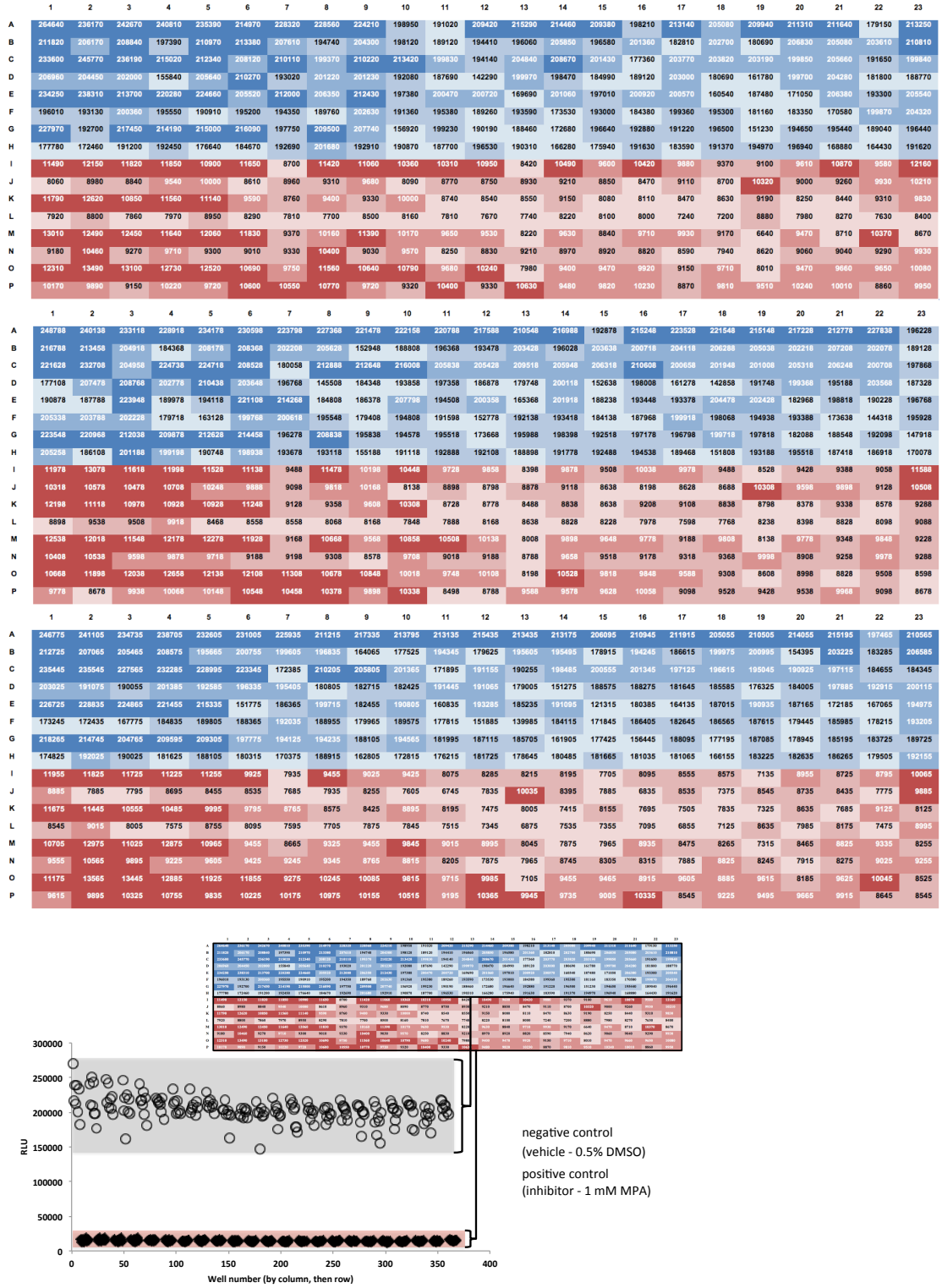


Fig. S1. Z'-factor calculation